Title

Serotonin receptors contribute to dopamine depression of lateral inhibition in the nucleus accumbens

Journal

Cell Reports, 39(6)

ISSN

2639-1856

Authors

Burke, Dennis A
Alvarez, Veronica A

Publication Date

2022-05-01

DOI

10.1016/j.celrep.2022.110795

Peer reviewed

HHS Public Access

Author manuscript

Cell Rep. Author manuscript; available in PMC 2022 June 07.

Published in final edited form as:

Cell Rep. 2022 May 10; 39(6): 110795. doi:10.1016/j.celrep.2022.110795.

Serotonin receptors contribute to dopamine depression of lateral inhibition in the nucleus accumbens

Dennis A. Burke[1,2], **Veronica A. Alvarez**[1,3,4,5,*]

[1]Laboratory on Neurobiology of Compulsive Behaviors, NIAAA, National Institutes of Health, Bethesda, MD 20892, USA

[2]Department of Neuroscience, Brown University, Providence, RI 02912, USA

[3]Intramural Research Program, NIDA, NIH, Baltimore, MD 21224, USA

[4]Center on Compulsive Behaviors, National Institutes of Health, Bethesda, MD 20892, USA

[5]Lead contact

SUMMARY

Dopamine modulation of nucleus accumbens (NAc) circuitry is central to theories of reward seeking and reinforcement learning. Despite decades of effort, the acute dopamine actions on the NAc microcircuitry remain puzzling. Here, we dissect out the direct actions of dopamine on lateral inhibition between medium spiny neurons (MSNs) in mouse brain slices and find that they are pathway specific. Dopamine potently depresses GABAergic transmission from presynaptic dopamine D2 receptor-expressing MSNs (D2-MSNs), whereas it potentiates transmission from presynaptic dopamine D1 receptor-expressing MSNs (D1-MSNs) onto other D1-MSNs. To our surprise, presynaptic D2 receptors mediate only half of the depression induced by endogenous and exogenous dopamine. Presynaptic serotonin 5-HT1B receptors are responsible for a significant component of dopamine-induced synaptic depression. This study clarifies the mechanistic understanding of dopamine actions in the NAc by showing pathway-specific modulation of lateral inhibition and involvement of D2 and 5-HT1B receptors in dopamine depression of D2-MSN synapses.

In brief

*Correspondence: alvarezva@mail.nih.gov.

AUTHOR CONTRIBUTIONS

Conceptualization and methodology, D.A.B. and V.A.A.; investigation, validation, and analysis, D.A.B.; writing, D.A.B. and V.A.A.; funding, resources, and supervision, V.A.A.

SUPPLEMENTAL INFORMATION

Supplemental information can be found online at https://doi.org/10.1016/j.celrep.2022.110795.

DECLARATION OF INTERESTS

The authors declare no competing interests.

INCLUSION AND DIVERSITY

We worked to ensure sex balance in the selection of non-human subjects. One or more of the authors of this paper self-identifies as an underrepresented ethnic minority in science. While citing references scientifically relevant for this work, we also actively worked to promote gender balance in our reference list.

Burke and Alvarez find that, in the nucleus accumbens, dopamine depresses or potentiates lateral inhibition between projection neurons, depending on the specific synapses isolated. Dopamine depression of D2-MSN GABA transmission involves activation of 5-HT1B receptors, suggesting that cross-talk between monoamines and receptors plays a role in accumbens circuit function.

Graphical Abstract

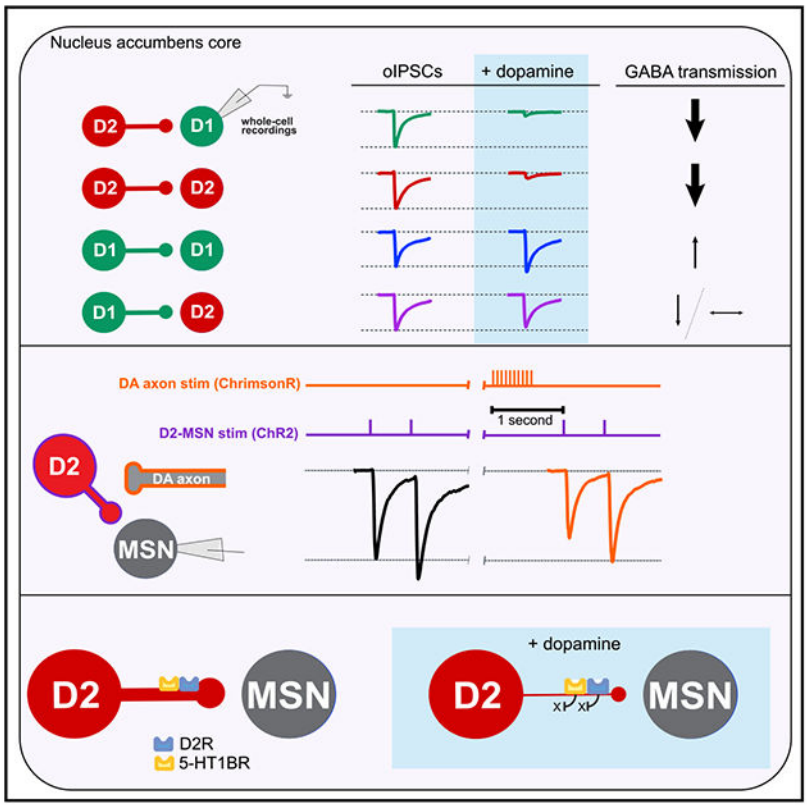

INTRODUCTION

Monoamine neuromodulators, such as dopamine (DA) and serotonin (5-HT), are found in the central nervous system of all vertebrates (Azmitia, 2007; Barron et al., 2010). These monoamines have evolved from a common origin, which is reflected in shared molecules used for loading of synaptic vesicles and for monoamine degradation. The common evolutionary origin is also evident in the high degree of sequence homology found in their receptors (Le Crom et al., 2003; Yamamoto and Vernier, 2011). Their divergence across the phylogeny has allowed monoamines to play a central role in regulation of diverse brain functions critical for survival, including sensory perception, motor control, and emotional regulation.

The nucleus accumbens (NAc), part of the ventral striatum, receives some of the highest DA innervation in the mammalian brain. Acting as a limbic-motor interface, the NAc drives motivated behaviors that are critical for survival, from flexible approach and reward seeking

or punishment avoidance to reinforcement learning. DA modulation of NAc circuitry is central to all current theories of how the NAc integrates cognitive and emotional information to drive behavior (Floresco, 2015; Ikemoto and Panksepp, 1999; Mogenson et al., 1980; Nicola, 2007; Pennartz et al., 1994). The NAc projection neurons, known as medium spiny neurons (MSNs), release GABA and neuropeptides. They receive excitatory inputs from the prefrontal cortex, thalamus, amygdala, and hippocampus that encode limbic and cognitive information (Britt et al., 2012). MSNs integrate these inputs and their information to help orchestrate the motor patterns that drive the aforementioned behaviors. As a neuromodulator, DA is thought to shape the integration of afferent information by modifying the cell excitability and synaptic transmission in the NAc microcircuitry (Burke et al., 2017; Tritsch and Sabatini, 2012).

The timescale of DA actions and whether DA signals for movement, motivation, salience, learning, or a combination of these functions is still debated (Berke, 2018; Berridge, 2007; Bromberg-Martin et al., 2010; Coddington and Dudman, 2019; Hamid et al., 2015; Kim et al., 2020; Lloyd and Dayan, 2015; Salamone and Correa, 2012; Schultz, 2016). Here we argue that the exact role of DA in the NAc remains unresolved in part because we still lack a complete understanding of DA modulation of NAc microcircuitry. Understanding the acute actions of DA at the cellular and synaptic level will reveal the circuit mechanisms underlying the cognitive and motivational processing that takes place in the NAc.

A powerful way by which DA is poised to shape afferent integration in the NAc is by modulating the extent of local inhibition. MSNs extend a wide network of local collateral axons in addition to their long-range projections to the targets outside of the striatum. These local axon collaterals form GABA synapses onto neighboring MSNs in the NAc and provide a powerful source of lateral inhibition among MSNs (Burke et al., 2017; Chang and Kitai, 1985; Czubayko and Plenz, 2002; Taverna et al., 2004; Tunstall et al., 2002). Previous work from our lab and others has demonstrated that this local network of inhibitory synapses between MSNs can suppress MSN excitability and output, regulating locomotion, the behavioral response to cocaine, and flexible goal-directed learning (Dobbs et al., 2016; Lemos et al., 2016; Matamales et al., 2020).

The acute actions of DA on NAc lateral inhibition remain unclear. Neither the net effect of DA nor the identity of receptors involved has been fully identified. In the NAc, DA receptors are expressed on a variety of inputs and cell types, including MSNs, which can be segregated into D1 receptor (D1R)-expressing direct pathway MSNs (D1-MSNs) and D2 receptor (D2R)-expressing indirect pathway MSNs (D2-MSNs). Although many earlier reports suggest that DA inhibits GABA synapses in the NAc through $G_{s/olf}$-coupled D1Rs and not through $G_{i/o}$-coupled D2Rs (Hjelmstad, 2004; Nicola and Malenka, 1997; Pennartz et al., 1992; Taverna et al., 2005), others have suggested that DA depresses lateral inhibition in MSNs through D2R activation (Kohnomi et al., 2012). These discrepancies may result from multiple factors: (1) a combination of direct and indirect effects of DA on the NAc circuitry (Corkrum et al., 2020); (2) a lack of selectivity in drugs used to target DA receptors (Millan et al., 2001); or (3) the ambiguous nature of the synapses examined, such as the unidentified MSN subtype recorded from and the lack of specificity in the stimulated GABA inputs. Over the past decades, transgenic mice have allowed discrimination of genetically

identified cells in the slice and selective pathway stimulation with channelrhodopsin (ChR2) or paired recordings. Using these tools, recent studies have shown that D2Rs depress GABA transmission from D2-MSNs, whereas D1Rs facilitate GABA transmission from D1-MSNs in the dorsal striatum (Tecuapetla et al., 2009; Wei et al., 2017), and that in the NAc, D2Rs depress D2-MSN→D1-MSN synapses (Dobbs et al., 2016). These studies suggest complex DA modulation of NAc lateral inhibition, which may depend on the specific synaptic partners. Using bath application pharmacology, none of these studies addressed the time course of DA actions on NAc lateral inhibition.

Thus, many questions remain unanswered. Does DA differentially modulate NAc lateral inhibition depending on the precise pre- and postsynaptic MSN subtype? Which receptors are involved in DA modulation of NAc lateral inhibition? What is the timescale of DA actions on lateral inhibition? In this study, we address these questions using transgenic mice and optogenetics. Specifically, we sequentially isolate the different synaptic connections between MSN subtypes that comprise the network of lateral inhibition and test how DA (endogenously released or exogenously applied) affects synaptic transmission using whole-cell recordings and optogenetic stimulation. We find that DA has fast and potent effects on lateral inhibition that differ depending on whether D1-MSNs or D2-MSN synaptic terminals are stimulated. DA potentiates GABA transmission from D1-MSN synapses onto other D1-MSNs and depresses transmission from D2-MSN synapses. Surprisingly, a significant portion of the depression induced by exogenously applied DA requires activation of 5-HT1B receptors (5-HT1BRs). This study provides crucial insight into DA's role in modulating NAc output and, in turn, motivated behavior by facilitating a better understanding of the acute modulation of this network of lateral inhibition by DA.

RESULTS

DA potentiates D1-MSN → D1-MSN synapses and depresses D2-MSN → D1-MSN synapses

We began by probing the actions of exogenous applied DA onto this local network of GABA synapses formed by axon collaterals from D1-MSNs and D2-MSNs onto D1-MSNs (Figure 1A). To record D1-MSN → D1-MSN synapses in the NAc core, D1-MSNs were transduced with Cre-dependent ChR2-eYFP through intra-NAc viral vector injection in double-transgenic Drd1-Cre;Drd1a-TdTomato mice (Figure 1B). Postsynaptic D1-MSNs were identified based on red fluorescence, and putative D2-MSNs were identified as unlabeled. In *ex vivo* brain slices, we performed whole-cell voltage-clamp recordings from tdTomato-expressing D1-MSNs while stimulating axons from D1-MSNs with brief light pulses (Figure 1D). Optogenetic evoked inhibitory postsynaptic currents (oIPSCs) were recorded until reaching a stable 10-min baseline period, after which DA was applied via bath perfusion. A concentration of 30 μM was chosen because it is within the range of concentrations reached at synapses following electrically stimulated DA release (Marcott et al., 2014; Patriarchi et al., 2018). In the presence of DA, GABA transmission at D1-MSN → D1-MSN synapses showed a small but significant potentiation to 111% ± 3% of baseline ($p < 0.01$; Figures 1D, 1E, and 1H; full statistics in Table S1). Note that, under these conditions, where the same MSN subtype recorded was also stimulated, optogenetic stimulation resulted in a combined oIPSC and direct ChR2-mediated current in the recorded

cell. In these cases, the ChR2 current was pharmacologically isolated from the synaptic current at the end of the experiment by applying GABA-A receptor blockers, and it was subtracted from the oIPSC. All measurements reported here are from the subtracted oIPSCs (STAR Methods; Figure S1).

To assess DA effects on D2-MSN → D1-MSN synapses, D2-MSNs were transduced with Cre-dependent ChR2-eYFP through intra-NAc viral vector injection in Adora2a-Cre;Drd1-tdTomato mice (Figure 1C). The same concentration of DA (30 μM) now significantly depresses GABA transmission to 14% ± 2% of baseline ($p < 0.0001$; Figures 1D, 1E, and 1H). This pronounced suppression of GABA transmission from D2-MSN inputs contrasted with the potentiation observed at D1-MSN → D1-MSN synapses ($p < 0.0001$; Figure 1H).

DA modulation of D1-MSN transmission depends on the postsynaptic target

We next assessed DA's effect when activating inputs from other D2-MSNs. We found that DA also depressed D2-MSN → D2-MSN GABA transmission to 16% ± 3% of baseline ($p < 0.0001$; Figure 1H). There was no significant difference in the degree of DA depression at D2-MSN → D1-MSN synapses and D2-MSN → D2-MSN synapses ($p = 0.99$; Figures 1F–1H). Conversely, when activating D1-MSN→D2-MSN synapses, application of DA resulted in no significant change in GABA transmission, just a trend toward a decrease (92% ± 4% of baseline after DA, $p = 0.08$; Figures 1F–1H). This result contrasts with the potentiation seen at D1-MSN→D1-MSN synapses. Thus, DA differentially affects GABA transmission at D1-MSN synapses, depending on the postsynaptic target, whereas DA suppresses synaptic transmission from D2-MSNs independent of the postsynaptic MSN target.

DA modulation of D2-MSN transmission depends on a presynaptic mechanism

So far, we found that DA acutely and equally depresses transmission from indirect pathway D2-MSNs onto neighboring D1-MSNs and D2-MSNs. This observation suggests that DA has a presynaptic site of action at D2-MSNs, where activation of presynaptic D2R decreases the probability of neurotransmitter release from D2-MSNs, which agrees with previously published data from the dorsal striatum (Guzmán et al., 2003; Tecuapetla et al., 2009). To examine this issue more closely in our NAc preparation, we analyzed the percent coefficient of variation (CV) of the oIPSC amplitudes during the baseline period and after DA application. The CV of IPSC amplitudes varies as a function of the presynaptic probability of transmitter release. Therefore, a decrease in oIPSC amplitude with a concomitant increase in the CV, and vice versa, suggests a presynaptic mechanism underlying the change in amplitude. Indeed, we found a significant increase in CV at both synapses with presynaptic D2-MSNs, from a CV of 20% ± 1.2% before to 83% ± 10% after DA in D2-MSN→D1-MSN synapses and from 14% ± 3% to 49% ± 9% after DA in D2-MSN→D2-MSN synapses ($p = 0.001$ and $p < 0.05$; Figure 1I). The CV at D1-MSN → D1-MSN synapses changed from 18% ± 2.5% to 14% ± 1.5% after DA and at D1-MSN→D2-MSN synapses from 10% ± 1.2% to 11% ± 1.1% after DA. In both cases, the CV changes by DA were not significant ($p = 0.16$ and $p = 0.38$, respectively; Figure 1I), suggesting that DA's effects on D1-MSN synapses are not presynaptically mediated. However, in both cases, the change in oIPSC amplitude is modest, and this could preclude us from detecting a CV change in this dataset. Thus, the observed CV changes when transmission was driven from

presynaptic D2-MSNs are largely consistent with a presynaptic site of action of DA at D2-MSN→MSN synapses, which is likely to involve a decrease in probability of GABA release from D2-MSN terminals.

Endogenously released DA from midbrain axon terminals depresses lateral inhibition from D2-MSNs

Although bath application of DA allows control over the pharmacology, the temporal and spatial profile of DA signaling evoked by bathing the entire slice for minutes at a time is likely very different from the conditions experienced by DA receptors *in vivo*. Thus, we next tested whether DA released from midbrain DA neuron axons modulates D2-MSN lateral inhibition.

Double transgenic/knockin mice with Cre expression in striatal D2-MSNs and midbrain DA neurons were transduced with Cre-dependent ChR2-eYFP in the NAc, as in previous experiments, and Cre-dependent ChrimsonR-tdTomato in midbrain DA neurons that project to the NAc (Figure 2A). Using fast scan cyclic voltammetry (FSCV) to detect DA, we confirmed that ChrimsonR stimulation (single and trains of light pulses) evoked DA concentration transients in the NAc core (Figures 2B, S2A–S2C, and S1D). Amplitudes of DA transients were relatively stable when evoked by a train of pulses every 2 min (10th/first amplitude = 0.89; Figure S2E). To evoke GABA release from D2-MSNs, ChR2 was activated with 405 nm to minimize spectral overlap with ChrimsonR, and pulse width and power were optimized to avoid triggering DA release (Figure S2F). A stable 10-min baseline of evoked oIPSCs was recorded from unlabeled MSNs in the NAc core while stimulating D2-MSN axon collaterals (paired pulses, 405 nm, 50-ms interval, every 20 s; Figure 2C). DA release was evoked every 2 min with ChrimsonR stimulation of DA axons (10 pulses at 20 Hz, 620 nm). The train started 1 s before GABA release stimulation and led to a reproducible reduction in amplitude of ~25% that recovered within 1 min (Figures 2D and 2E). Averaged oIPSC amplitudes before and after DA neuron stimulation show that stimulation of DA neuron axons caused a significant depression to 77% ± 2% of the pre-stimulation value ($p < 0.0001$; Figures 2F and 2G). The amplitude recovered within 1 min. The CV of oIPSC amplitude increased from 17% ± 3% before to 29% ± 4% after stimulation of DA neurons ($p < 0.01$; Figure S3A). The paired pulse ratio (PPR; 50-ms interval) of IPSCs also increased from 1.8 ± 0.3 to 2.6 ± 0.7 immediately after DA neuron stimulation ($p < 0.01$; Figure S3B). The increases in CV and PPR are consistent with a presynaptic site of action and suggest that the depression is mediated by lowering the probability of GABA release at D2-MSN terminals. These results indicate that stimulation of DA neuron axons in the NAc is sufficient for acutely and reversibly depressing GABA transmission from D2-MSNs on a timescale of milliseconds to seconds. We speculate that this acute suppression of lateral inhibition among MSNs would lead to transient changes in the threshold for MSN excitability, creating a short time window for amplification of incoming excitatory inputs to the NAc to modulate ongoing activity and set the stage for plasticity.

Cocaine prolongs synaptic depression by endogenously released DA, which is partially insensitive to D2R antagonists

In search of evidence that DA mediates ventral tegmental area (VTA) terminal-induced depression, we tested the effect of cocaine, a blocker of monoamine transporters. We reasoned that blocking DA reuptake with cocaine would prevent DA clearance and increase DA concentration near the release site. If the depression is mediated by DA, then cocaine would prolong the depression of GABA transmission but would have no effect if the depression is mediated by glutamate or GABA, two other neurotransmitters known to be co-released from midbrain DA neuron axons (Adrover et al., 2014; Stuber et al., 2010; Tecuapetla et al., 2010; Tritsch et al., 2012). Application of 3 μM cocaine significantly increased the magnitude and time course of depression after DA stimulation ($p < 0.0001$; Figure 2F). First, we observed that cocaine produced a lasting depression of oIPSC amplitudes, causing the oIPSC to remain significantly depressed after each DA stimulation train ($p < 0.0001$; Figures 2F and S3C). This effect of cocaine raised concerns about possible occlusion of the acute effect of DA neuron stimulation. To circumvent this concern and compare the acute effects with and without cocaine, the data were normalized to the pre-DA stimulation amplitude of each condition (Figures 2G and 2H). DA neuron stimulation in the presence of cocaine produced significant acute depression of D2-MSN IPSCs to 82% ± 3% of the pre-stimulation amplitude ($p < 0.01$; Figure 2G). As predicted, cocaine also prolonged depression of oIPSC amplitude, which remained lower even 21 s after DA neuron stimulation, significantly different from the no-cocaine condition ($p < 0.05$; Figure 2H).

We next hypothesized that DA D2Rs, likely expressed on D2-MSN terminals, were responsible for the synaptic depression of GABA transmission after stimulation of midbrain DA neuron axons. To test this hypothesis, slices were pretreated with the D2R-like antagonist sulpiride (10 μM) before applying cocaine and then stimulating DA neurons. Sulpiride significantly attenuated the acute effects of DA neuron stimulation compared with cocaine alone ($p < 0.05$; Figure 2I). However, to our surprise, a portion of acute depression persisted after DA neuron stimulation, where D2-MSN IPSC amplitude was reduced to 90% ± 4% of the pre-stimulation amplitude ($p < 0.05$; Figure 2G). These results suggest that DA D2Rs contribute to, but are only partially responsible for, the synaptic depression driven by DA neuron stimulation in the presence of cocaine.

DA depresses D2-MSN lateral inhibition via two mechanisms: D2R dependent and independent

Puzzled by the findings that the D2R-like antagonist sulpiride was unable to fully block the depression induced by endogenous neurotransmitter released from DA neurons in the presence of cocaine, we sought to validate the finding with exogenously applied DA. In brain slices pretreated with sulpiride (10 μM), exogenous application of DA (30 μM) was still able to significantly depress D2-MSN → D1-MSN transmission. oIPSC amplitude decreased to 49% ± 8% of baseline ($p < 0.01$; Figure 3A), about half the depression driven by DA in the absence of D2R antagonism. To validate the pharmacology, we next tested DA in brain slices from mice with targeted deletion of D2Rs from D2-MSNs (iMSN-Drd2 knockout [KO] mice: Adora2a-Cre;$D2^{loxP/loxP}$ mice) (Lemos et al., 2016). In slices from these cell-specific KO mice, DA depressed D2-MSN → MSN oIPSC amplitude to 50% ±

8% of baseline ($p = 0.001$; Figure 3B). The magnitude and time course of DA depression were similar and overlapping in wild-type (WT) slices pretreated with sulpiride and slices from mice lacking D2Rs in D2-MSNs ($p = 0.99$; Figure 3C). Under both conditions, depression by DA was significantly attenuated compared with untreated WT slices (WT + sulpiride, $p < 0.05$; iMSN-Drd2KO, $p < 0.01$; Figure 3C). Together with the previous results from midbrain neuron stimulation, these experiments provide further evidence that DA depresses D2-MSN lateral inhibition through two processes: direct activation of presynaptic D2Rs and a D2R-independent mechanism.

DA depression involves another G-protein-coupled receptor with a 4-fold shift in IC_{50}

To address the D2R-independent depression, we sought to determine whether the remaining depression by DA involves a class of G-protein-coupled receptors (GPCRs). N-ethylmaleimide (NEM) is a sulfhydryl alkylating agent that uncouples pertussis toxin-sensitive Gi/o proteins from their receptors (Shapiro et al., 1994). In slices from iMSN-Drd2KO mice pretreated with NEM (50 μM), D2R-independent depression was significantly attenuated compared with untreated slices ($p < 0.0001$ versus WT + sulpiride and versus iMSN-Drd2KO; Figure 3C). In fact, in NEM-treated iMSN-Drd2KO slices, DA failed to depress D2-MSN → MSN GABA transmission (114% ± 118% of baseline, $p = 0.20$; Figure S4A), which suggests that the D2R-independent depression by DA is mediated by Gi/o signaling.

We next assessed the concentration dependence of this remaining GPCR-dependent depression by DA. DA concentrations ranging from 100 nM to 300 μM were tested at D2-MSN→MSN synapses in iMSN-Drd2KO mice. We found that D2R-independent DA depression is concentration dependent at these synapses, and the IC_{50} was estimated to be 37 μM (Figure 3D; curve fit data in Table S1). In WT Adora2a-Cre mice, the concentration-response curve for DA depression at these synapses was shifted leftward 4-fold compared with that observed in iMSN-Drd2KO mice, with a significantly different estimated IC_{50} of 9.1 μM DA ($p < 0.001$, extra-sum-of-squares F test). Thus, we found D2R-independent depression to require G-protein activity, to be concentration dependent, and to be active at low micromolar concentrations of DA.

A presynaptic mechanism for D2R-independent depression by DA

Two main pieces of evidence support a presynaptic mechanism for D2R-independent depression by DA. First, DA significantly increased the CV of the oIPSC amplitude in WT slices treated with sulpiride (from 17% ± 2% to 36% ± 9% after DA, $p < 0.05$) as well as in slices from iMSN-Drd2KO mice (from 17% ± 1% to 32% ± 4% after DA, $p < 0.05$; Figure 3E). Second, in WT slices treated with sulpiride, DA significantly increased the PPR (50 ms interval) of oIPSCs compared with the ratios at baseline (from 0.59 ± 0.05 to 0.85 ± 0.03 after DA, $p < 0.05$; Figure 3F), consistent with a presynaptic mechanism. These findings suggest that DA decreases the probability of GABA release from the synaptic terminals. However, neither result excludes an additional postsynaptic change in GABA receptor signaling after DA. Thus, we directly tested the effect of DA on GABA receptor-mediated currents evoked by photo-uncaging of Rubi-GABA onto the slice (Rial Verde et al., 2008).

Rubi-GABA is a chemically caged GABA compound that is uncaged to release GABA in the presence of blue light. We bath-applied Rubi-GABA (10 μM) to brain slices from Drd1-tdTomato mice and recorded from D1-MSNs. Blue laser stimulation was used to uncage Rubi-GABA and stimulate GABA currents on D1-MSNs without a contribution from presynaptic MSNs. In the presence of DA, the amplitude of the uncaged IPSC showed a small but significant increase to 107% ± 2% of baseline ($p < 0.05$; Figure 3G). This small but significant increase in GABA uncaging currents by DA (107% ± 2%) is comparable with the potentiation by DA at D1-MSN→D1-MSN synapses (111% ± 3%), suggesting that DA-mediated potentiation at D1-MSN→D1-MSN synapses is mediated by activation of receptors located in the postsynaptic D1-MSN (Figures 1E, 1H, and 1I). At D2-MSN → MSN synapses, however, DA depressed transmission. Because DA did not replicate the depression when currents were evoked by uncaged GABA bypassing the presynaptic terminal, these results are consistent with a presynaptic site of action for DA at D2-MSN → MSN synapses for both the D2R-independent as well as D2R-dependent depression.

Activation of D2Rs in presynaptic D2-MSNs depresses MSN lateral inhibition

To understand the more tractable D2R-mediated inhibition by DA, we next used a full agonist at D2-like receptors. We directly assessed how D2R activation with quinpirole affected MSN → MSN transmission at the four possible combinations of synaptic partners: D2-MSN→D1-MSN, D2-MSN→D2-MSN, D1-MSN→D2-MSN, and D1-MSN→D1-MSN.

At D2-MSN → D1-MSN synapses, in which D2Rs are expressed only at the presynaptic site, 1 μM quinpirole caused a significant depression of GABA transmission to 44% ± 3% of baseline. As expected, quinpirole also increased the CV of the oIPSC amplitudes (from 21% ± 3% to 47% ± 6%, $p < 0.0001$; Figure 4F). To our surprise, the quinpirole-induced depression recovered to only 76% ± 4% of baseline upon washout and further application of the D2-like receptor antagonist sulpiride (1 μM, all $p < 0.0001$; Figure 4A). In slices pre-treated with sulpiride, quinpirole had no effect on synaptic transmission (sulpiride baseline, 100% ± 2%; +quinpirole, 101% ± 4%; $p = 0.88$; Figure S5), suggesting that quinpirole induces some degree of long-lasting depression at these synapses.

At D2-MSN → D2-MSN synapses, in which pre- and postsynaptic neurons express D2Rs, quinpirole again depressed GABA transmission to 37% ± 5% of baseline. Interestingly, quinpirole depression was fully reversed by sulpiride application at these synapses (94% ± 7% of baseline, $p < 0.0001$ for baseline versus quinpirole [quin] and quin versus sulpiride [sulp], $p = 0.65$ for baseline versus sulp; Figure 4B). Apart from the recovery, there was no significant difference in acute quin-mediated depression of D2-MSN → D1-MSN and D2-MSN → D2-MSN synapses ($p = 0.54$; Figure 4E). In addition, quin increased the CV of oIPSC amplitudes at D2-MSN → D2-MSN synapses (baseline, 23% ± 3%; quin, 49% ± 3%; $p = 0.001$; Figure 4F), further suggesting that D2R-mediated depression is presynaptically mediated.

At D1-MSN → D2-MSN synapses, in which D2Rs are only expressed in postsynaptic neurons, quin application caused a very small but significant depression of GABA transmission to 91% ± 2% of baseline. The small depression was reversed by sulp to 96%

± 3% of baseline ($p < 0.05$ for baseline versus quin, $p > 0.16$ quin versus sulp and baseline versus sulp; Figure 4C), and it was not accompanied by changes in CV (from 13% ± 2% to 14% ± 3% after quin, $p = 0.31$; Figure 4F).

At D1-MSN → D1-MSN synapses, quin and sulp application had no effect on GABA transmission (from baseline; quin, 102% ± 3%; sulp, 104% ± 8%; $p = 0.95$; Figure 4D). The lack of effect was expected because neither presynaptic nor postsynaptic neurons should express D2Rs. Despite reports of a small subpopulation of MSNs that coexpresses D1 and D2Rs in the NAc core (~6%; Bertran-Gonzalez et al., 2008) or D1 and D3 receptors (mainly the NAc medial shell; Ridray et al., 1998), our finding here suggests that these subpopulations are unlikely to play a large functional role at these collateral synapses.

Thus, we conclude that quin mainly depresses transmission at synapses where presynaptic MSNs express D2Rs. The most parsimonious interpretation is that quin acts directly on D2Rs on D2-MSN axons. However, other cell types in the NAc also express D2Rs, including cholinergic interneurons, which have been shown to indirectly modulate synapses onto MSNs in slices (Augustin et al., 2018; Francis et al., 2019) and could therefore play a role in D2R-mediated depression of lateral inhibition. Although not completely excluding this possibility, the lack of depression at D1-MSN→D1-MSN synapses suggests that, in our preparation, D2R depression is mediated through D2Rs on D2-MSNs.

D2R-mediated depression accounts for half of the DA effect

The magnitude of depression by 30 μM DA is greater than that by 1 μM quin (86% ± 2% versus 56% ± 3% depression) (Figures 1E, 1H, and 4A). 3 and 10 μM quin depressed to the same extent as 1 μM (47% ± 10%, 48% ± 4%, and 44% ± 3% of baseline, respectively; Figure 4G), indicating that ~52%–56% is the maximal depression mediated by D2R at these synapses. However, DA depresses GABA transmission to a greater extent; 30 μM reduces the amplitude to 14% ± 2% of baseline and 100 μM to 7.4% ± 4% of baseline ($p < 0.0001$ versus 1 μM quin; Figure 4G). Thus, DA depression is significantly larger than the maximal quin depression, consistent with our previous findings indicating a second mechanism of action for DA that is independent of D2Rs.

D1Rs are not involved in D2R-independent depression of D2-MSN lateral inhibition by DA

D1Rs are other well-known targets of DA that are highly expressed in the NAc. We examined whether D1R antagonism could attenuate D2R-independent depression using slices from iMSN-Drd2KO mice where the D2R-independent depression can be isolated. In the presence of the D1-like antagonist SCH23390 (2 μM), DA still depressed GABA transmission at D2-MSN → MSN to 51 % ± 7% baseline ($p < 0.01$; Figure 5A), similar to the no-antagonist condition and to 20 μM SCH23390 (32% ± 9% baseline, $p = 0.38$; Figure 5B). We also tested a cocktail of DA receptor antagonists containing another high-potency D1-like antagonist, SKF83566 (1 μM); the D2-like antagonist sulp (10 μM); and the D4R antagonist L-745870 (1 μM). DA caused a similar depression in the presence of this antagonist cocktail (56% ±5% baseline; Figure 5B). Last, we tested whether the selective full D1-like agonist SKF81297 could mimic D2R-independent depression by DA. SKF81297 (10 μM) had no effect on D2-MSN lateral inhibition (93% ± 5% baseline, p =

0.29; Figure 5C). These results rule out involvement of any known DA receptor types in the D2R-independent portion of DA depression of D2-MSN lateral inhibition.

5-HT1BRs mediate part of DA depression of D2-MSN lateral inhibition

Some studies have reported promiscuous binding and activation among monoamine receptors (Bhattacharyya et al., 2006; Conductier et al., 2011; Guiard et al., 2008; Oz et al., 2003; Root et al., 2015; Sánchez-Soto et al., 2018). Because α2-adrenergic receptors (α-ARs) and 5-HT1 BRs are expressed in the NAc and can act as heteroreceptors that presynaptically depress transmitter release (Matsui and Alvarez, 2018; Puighermanal et al., 2020; Tiger et al., 2018; Uhlén et al., 1997), we next tested whether antagonists for these receptors could block D2R-independent depression by DA in iMSN-Drd2KO mice. An α-AR cocktail consisting of yohimbine (3 μM), RX821002 (10 μM), and prazosin (100 nM) had no effect on D2R-independent depression (53% ± 7% baseline; ACSF versus α-AR cocktail, $p = 0.92$), whereas pretreatment with NAS-181, a selective 5-HT1BR antagonist, significantly attenuated DA depression (79% ± 3% baseline; ACSF versus NAS-181, $p < 0.01$; α-AR cocktail versus NAS-181, $p < 0.05$; Figures 6A and 6C). In addition, pretreatment with an antagonists for adenosine A1 and A2A, muscarinic, cannabinoid, GABA-B, opioid, histamine H3, mGluR group II, nicotinic, or other 5-HT receptors had no effect on the D2R-independent depression in slices from iMSN-Drd2KO mice ($p = 0.82$; Figure S6A). NAS-181 attenuated D2R-independent depression of D2-MSN lateral inhibition in WT (Adora2a-Cre) mice. In slices pretreated with sulp and NAS-181, DA depression (81% ± 10% baseline) was significantly attenuated compared with no antagonist treatment or sulp alone ($p < 0.01$ for NAS-181 + sulp versus sulp alone, NAS-181 + sulp versus no antagonist, sulp alone versus no antagonist; Figures 6B and 6D). To further validate this finding, we crossed mice with global deletion of 5-HT1BRs (5-HT1BKO) with Adora2a-Cre;D1-tdTomato mice to record D2-MSN→D1-MSN transmission. Again we observed attenuation of D2R-independent depression by DA (73% ± 4% baseline). The DA effect was reduced to the same extent in mice with genetic deletion of the 5-HT1BR as in WT slices pretreated with NAS-181 (NAS-181 + sulp versus 5-HT1BKO + sulp, $p = 0.77$; Figure 6D), which was also significantly different from WT slices pretreated with sulp (5-HT1BKO + sulp versus sulp alone, $p < 0.05$; Figure 6D), again suggesting that DA depresses lateral inhibition through D2Rs and 5-HT1BRs. These data offer strong evidence that activation of 5-HT1BRs is required for part of the DA depression of D2-MSN lateral inhibition.

We reasoned that direct activation of 5-HT1BR with a selective agonist should depress D2-MSN GABA transmission. We tested the 5-HT1B/1D selective agonist sumatriptan (1 μM) on D2-MSN→D1-MSN synapses in WT mice and, as predicted, found robust depression of oIPSC amplitudes to 40% ± 4% of baseline ($p < 0.0001$; Figure 6E). Addition of quin (1 μM) on top of sumatriptan further depressed oIPSC amplitudes to 14% ± 3% of baseline, significantly less than baseline ($p < 0.0001$) and sumatriptan alone ($p < 0.001$; Figure 6E). Combined sumatriptan and quin application depressed transmission to a greater extent than quin alone ($p < 0.001$; Figure 6F). These results are consistent with DA depressing D2-MSN lateral inhibition via combined actions on D2Rs and 5-HT1BRs.

D1-MSNs also express 5-HT1BRs (Sari et al., 1999), but DA produced no depression at D1-MSN→D1-MSN synapses (Figure 1H). We tested sumatriptan (1 μM) and found that it significantly depressed GABA transmission to 70% ± 5% of baseline at D1-MSN→D1-MSN synapses ($p < 0.01$, Figure S7A). This depression was significantly less than at D2-MSN→D1-MSN synapses ($p < 0.01$; Figure S7B), implying lower potency of 5-HT1BR at D1-MSN→D1-MSN synapses and providing a possible explanation for the lack of DA depression at these synapses.

DA depression through 5-HT1BRs is neither enhanced nor occluded by selective blockers of the 5-HT transporter

So far, our study cannot rule out an indirect mechanism for involvement of 5-HT1BRs in DA-mediated depression. For example, DA application might somehow elevate extracellular 5-HT concentrations in the slice by inducing 5-HT release or blocking 5-HT reuptake via the 5-HT transporter (SERT). To test these possibilities, we applied the selective 5-HT reuptake inhibitor citalopram (1 μM) (Matsui and Alvarez, 2018) to the slice before adding DA (30 μM) and recorded from D2-MSN→D1-MSN synapses in iMSN-Drd2KO mice. We predicted that, if DA is inducing 5-HT release by some indirect mechanism, citalopram will further enhance the 5-HT1B-mediated depression by DA. Alternatively, if DA is blocking 5-HT reuptake via SERT, causing an increase in extracellular 5-HT levels (the DA affinity for SERT is higher than 5-HT), citalopram will occlude 5-HT1B-mediated depression by DA.

The experiments first showed that citalopram alone caused a small but significant reduction in oIPSC amplitude to 88% ± 4% baseline ($p < 0.01$; Figure 7A), suggesting the presence of a 5-HT tone in the slice. Addition of DA to the slice in the presence of citalopram further decreased oIPSC amplitudes to 43% ± 4% baseline ($p < 0.0001$ for comparisons with baseline and citalopram alone; Figure 7A). The depression of lateral inhibition caused by combined citalopram and DA, however, was not significantly different from that of DA alone in iMSN-Drd2KO mice ($p = 0.52$; Figure 7B). Because citalopram neither amplifies nor occludes the DA effect on 5-HT1BRs when increasing the extracellular concentration of 5-HT, we conclude that it is unlikely that endogenous 5-HT is mediating the 5-HT1BR-dependent depression by DA. Thus, the most parsimonious explanation is that DA acts directly on 5-HT1BRs located in the presynaptic GABA terminals and activates these receptors to mediate a transient depression of synaptic transmission.

Regarding the remaining component of D2R-independent depression, the identity of the receptor(s) remains unclear. This remaining depression was insensitive to a range of antagonists (DAergic, adrenergic, muscarinic, nicotinic, GABA-B, cannabinoid, opioid, histamine, and adenosine as well as fast glutamate blockers present throughout this study; Figure S6A). However, our evidence suggests that a presynaptic (Figures 3E–3G) Gi/o-coupled receptor (Figure S4) mediates the remaining component of the depression.

Combined antagonists for 5-HT1BRs and D2Rs reverse and block the depression by endogenous DA in the presence of cocaine

D2R antagonism by itself was insufficient for blocking the acute depression induced by endogenous DA released using optogenetic stimulation of DA axons in the presence of cocaine (Figure 2G). Using a similar setup, we tested whether combined 5-HT1BR and D2R antagonists could completely block the acute depression. D2-MSNs and midbrain DA neurons were virally transduced with ChR2-eYFP and ChrimsonR-tdTomato, respectively, in Adora2a-Cre;DAT-Cre mice. As in the experiments shown in Figure 2, cocaine (3 μM) was included in the bath because it amplified the inhibition evoked by DA axon stimulation and validated the involvement of endogenous DA. We recorded oIPSCs in unlabeled MSNs to obtain a stable baseline before DA release was optogenetically evoked by train stimulation every 2 min for 20 min. Normalizing the oIPSC amplitudes to the pre-DA stimulation amplitudes and averaging epochs, we again found acute depression to 86% ± 3% baseline. The depression began 1 s after DA stimulation ($p < 0.01$ versus – 19 s), peaked at 21 s (70% ± 3% pre-stimulation, $p < 0.0001$ versus – 19 s; Figure 7D, blue), and reversed over the course of 1 min (Figure 7C, blue). We then applied sulp (10 μM) and NAS-181 (20 μM) together in the bath and allowed 5 min for the drugs to equilibrate. We found that the combination of antagonists for D2Rs and 5-HT1BRs completely blocked acute depression after endogenous DA release. The antagonist combination significantly attenuated acute depression at all time points after DA axon stimulation ($p < 0.01$ for 1–61 s; Figure 7C). In contrast to pre-antagonist application, there was no effect of DA axon stimulation on oIPSC amplitudes 1 s (99% ± 2% pre-stimulation, $p = 0.79$ versus – 19 s) or 21 s (104% ± 3%, $p = 0.24$ versus – 19 s) after stimulation compared with pre-DA stimulation amplitudes (Figure 7D, gray). Thus, the combined D2R and 5-HT1BR antagonists fully reverse acute depression of D2-MSN lateral inhibition by DA neuron stimulation in the presence of cocaine. These results strongly suggest that, in the presence of cocaine, the acute depression caused by endogenous DA release is mediated in part by 5-HT1BRs.

DISCUSSION

This study dissects out the modulatory role of the monoamine DA on local NAc GABA transmission, which provides a strong source of lateral inhibition among principal neurons. This topic has been addressed before, particularly in the dorsal striatum, but the results remained controversial and the interpretation puzzling. The present findings clarify the picture by showing that DA differentially modulates MSN→MSN lateral inhibition in a pathway-specific manner. DA greatly depresses GABA transmission from D2-MSNs to D1-MSNs and other D2-MSNs, whereas it has a small target-specific effect on D1-MSN transmission: small facilitation and depression at D1-MSN → D1-MSN and D1-MSN → D2-MSN, respectively. We postulate that DA depresses D2-MSN lateral inhibition via presynaptic receptors, likely expressed at synaptic terminals, whereas DA differential effects on D1-MSN lateral inhibition depend on postsynaptic receptors. We also found that DA released from the terminals of midbrain DA neurons produces transient and reliable depression of D2-MSN synapses within 1 s. This depression is prolonged by cocaine and only partially blocked by D2-like receptor antagonists in the presence of cocaine. To our surprise, a significant portion of exogenous DA-induced depression is mediated by

presynaptic 5-HT1BRs. Thus, the results from this study reveal that DA bidirectionally modulates lateral inhibition among MSNs via multiple monoamine receptors and that it does so in a fast and transient fashion, which is expected to have important implications for the excitability of MSNs and NAc output. These results provide crucial information for a full understanding of how DA shapes NAc circuitry to exert its known effects on motivated behavior.

Pathway specificity of DA actions

The pathway selectivity observed in the NAc is broadly in agreement with results from the dorsal striatum but with some differences. Researchers have consistently demonstrated that, in the dorsal striatum, DA mainly modulates GABA transmission presynaptically, depressing release from presynaptic D2-MSNs and facilitating release from presynaptic D1-MSNs (Guzmán et al., 2003; Tecuapetla et al., 2007, 2009; Wei et al., 2017). Although we did observe a potentiation at D1-MSN→D1-MSN synapses, we found no evidence of a presynaptic mechanism through the CV analysis. This could be due to the small effect size of the potentiation observed that prevents us from resolving differences in CV. Alternatively, the failure to detect a change in CV could be interpreted as evidence of a postsynaptic mechanism of DA in D1-MSN transmission. The latter is further supported by the fact that DA produced the same small potentiation on currents evoked by uncaging GABA on D1-MSNs. Last, the fact that DA has a different effect on D1-MSN→D2-MSN synapses also supports a postsynaptic site of action. These target-specific effects of DA have not been reported before. Given the relative scarcity of D1-MSN→D2-MSN synapses based on paired recording data (Planert et al., 2010; Taverna et al., 2008; Wei et al., 2017), it is not surprising that DA modulation of this specific synaptic pair has been less studied.

Our results also agree with previous reports that D2R activation depresses MSN→MSN synapses in the NAc (Dobbs et al., 2016; Kohnomi et al., 2012). Previously published results from the NAc, however, showed that DA depression of electrically stimulated GABA currents onto MSNs was blocked by D1-like but not D2-like receptor antagonists. DA depression was mimicked or occluded by D1-like agonists, which suggested that, in the NAc, DA depresses GABA transmission through D1Rs (Hjelmstad, 2004; Nicola and Malenka, 1997; Pennartz et al., 1992). Similarly, when using paired recordings from subtype-unidentified MSNs, Taverna etal. (2005) found that this synapse is depressed by DA and by a D1-like agonist. Electrical stimulation recruits a mixed population of axon terminals, both MSN subtypes, interneurons, and ventral pallidum (VP) back-projections, which complicates a direct comparison of results and might explain the difference. Differences in animal species (mouse versus rat) and the NAc subregions being recorded are other factors that may account for the apparent discrepancy between our and previous data using paired recording. For example, the NAc shell and core display heterogeneity in D1R signaling, DA transmission, and psychostimulant-induced adaptations (de Jong et al., 2019; Kourrich and Thomas, 2009; Saddoris et al., 2013; Corkrum et al., 2020 Kohnomi et al., 2012, 2017). There are reported differences in D1R and D2R signaling between the dorsal striatum and NAc shell (Gangarossa et al., 2013; Gerfen et al., 2008; Marcott et al., 2018). The evidence indicates that the NAc shell has distinctive properties and that the DA

effects on the NAc core assessed in this study are broadly similar to those described for the dorsal striatum.

Timescale of DA actions

This study found that DA released from midbrain VTA neurons depresses D2-MSN synapses on a millisecond-to-second timescale. The 20-s sampling interval for oIPSCs precluded us from determining the time course of this depression with higher time resolution. Future experiments and strategies will be needed to study the exact time course of the depression, including the time window between DA release and MSN GABA release that leads to maximal IPSC depression. The acute depression driven by DA neuron stimulation was rapid in onset, occurring within 1 s of DA stimulation. This depression is prolonged by cocaine. Our results add to accumulating evidence that DA release from midbrain projections in the striatum can exert effects on postsynaptic targets on subsecond timescales (Lahiri and Bevan, 2020; Marcott et al., 2014; Shin et al., 2017). Unlike the rapid effects of DA neuron stimulation on D1-MSN excitability in the dorsal striatum, which persist for minutes (Lahiri and Bevan, 2020), the depression of synaptic transmission observed here is transient and reversible within 1 min. This short-acting acute depression by endogenously released DA suggests a possible mechanism where DA, through disinhibition of neighboring MSNs (Dobbs et al., 2016), can transiently shape NAc circuitry to modulate moment-by-moment behavior to invigorate actions (Hamid et al., 2015; Nicola, 2010; Puryear et al., 2010; Roitman et al., 2004; Da Silva et al., 2018; Wang and Tsien, 2011). By increasing cell excitability through reduction of synaptic GABA, DA could lower the threshold for plasticity at a set of inputs whose activation are time locked to the DA signals (Reynolds et al., 2001). The plasticity-inducing effect of DA would then be selective for inputs arriving within an effective time range, whereas other inputs that are active before or after this time window would be unaffected. Under this hypothesis, the transient nature of the DA depression could then also assist in driving reinforcement learning. Interestingly, one recent study suggested a narrow time window (~1 s) in which DA signaling drives learning (Lee et al., 2020). Thus, by identifying the molecules and pathway specificity of DA control over GABA inhibition among NAc MSNs, the current study offers possible synaptic mechanisms underlying the known role of DA in plasticity and learning (Augustin et al., 2018; Goto and Grace, 2005; Shindou et al., 2019; Steinberg et al., 2013; Yagishita et al., 2014).

Involvement of 5-HT1BRs

A critical revelation from this study is the involvement of 5-HT1BRs in DA actions on synapses. About half of the exogenous DA-induced depression of the lateral inhibition from D2-MSN is driven by activation of presynaptic D2Rs, as expected, given the known role of D2Rs in depressing GABA release in the striatum and NAc (Dobbs et al., 2016; Tecuapetla et al., 2009). To our surprise, however, a significant portion of DA-induced depression is insensitive to antagonists for all known types of DA receptors. This resistant portion of DA depression is largely blocked by a 5-HT1BR antagonist and genetic KO of the 5-HT1BR gene. We also found that DA axon stimulation induces a transient depression of D2-MSN lateral inhibition that is enhanced by cocaine and not fully blocked by a D2R antagonist.

Combined application of D2R and 5-HT1BR antagonists fully reverses and prevents acute depression by DA neuron stimulation in the presence of cocaine.

Cooperative interactions

Our findings raise the possibility of cooperative interactions between D2Rs and 5-HT1BRs, which both depress lateral inhibition in the NAc. Agonists for 5-HT1BRs and D2-like receptors together depressed transmission to a greater extent than D2-like receptors alone. This cooperative depression seems likely to be relevant *in vivo* in the presence of cocaine, which blocks reuptake of both monoamines. With cocaine, roughly half of the acute synaptic depression caused by DA neuron stimulation is mediated by 5-HT1BRs. Our findings do not completely rule out the involvement of D2R-5-HT1BR heterodimers in this depression. However, we consider this possibility highly unlikely because the DA depression is preserved in animals lacking D2Rs in D2-MSNs. The 5-HT1B antagonist also blocks DA-mediated depression in iMSN-Drd2KO mice, which lack D2Rs.

Monoamine receptor cross-talk and pharmacology

Early efforts to characterize the rat 5-HT1BR suggested that it displays low affinity for DA (Hoyer, 1988; Markstein et al., 1986; Peroutka and Snyder, 1979). However, the lack of selective blockers for 5-HT1BRs at the time cast doubt over the interpretation of these experiments (Schoeffter and Hoyer, 1989; Van Wijngaarden et al., 1990). 5-HT receptor pharmacology is complex, in part because of profound heterogeneity among species (McCorvy and Roth, 2015), which is particularly relevant to our findings. For example, human and rat 5-HT1BRs share more than 93% sequence homology and have similar affinity for 5-HT. However, a single amino acid substitution in the human threonine355 for asparagine351 in rats confers rat 5-HT1BRs with 100-to 1,000-fold greater affinity for adrenergic antagonists and altered binding to classic 5-HT ligands (Adham et al., 1994; Metcalf et al., 1992; Oksenberg et al., 1992). The mouse 5-HT1BRs carries the same asparagine residue and reportedly has a similar pharmacology as the rat 5-HT1BR (Maroteaux et al., 1992). Less is known about mouse 5-HT1BRs because current efforts regarding therapeutic drug development and pharmacology have largely focused on human 5-HT1BRs (Rodríguez et al., 2014). Our current findings point to a need for further examination of mouse 5-HT1BR pharmacology. D2-MSNs express 5-HT1BRs (Puighermanal et al., 2020). Similar to D2Rs, 5-HT1BRs are GPCRs that couple to Gi/o proteins and are expressed on presynaptic terminals, where they mediate heterosynaptic depression of neurotransmitter release (Tiger et al., 2018). We found that the 5-HT1B/1D agonist sumatriptan depressed D2-MSN→D1-MSN synapses as well as D1-MSN→D1-MSN synapses (Figures 6E and S7A), consistent with recent work (Pommer et al., 2021). In addition, in the striatum, 5-HT1BRs are expressed on glutamate inputs and cholinergic interneurons, where they can depress glutamate and acetylcholine release (Dölen et al., 2013; Mathur et al., 2011; Matsui and Alvarez, 2018; Virk et al., 2016).

Because of their common evolutionary history, monoamine transmitters share many of the release and degradation machinery, including vesicular monoamine transporter 2 and monoamine oxidase (Yamamoto and Vernier, 2011). There are many reports of cross-talk between monoamines, including reuptake transporters (Larsen et al., 2011; Morón et al.,

2002; Shen et al., 2004) and receptors (Conductier et al., 2011; Comil and Ball, 2008; Cornil et al., 2008; Guiard et al., 2008; Lanau et al., 2002; Root et al., 2015; Yang et al., 2014; Zhang et al., 2004). There are also reports that DA decreases GABA release in the striatum through α2 receptors (Zhang and Ordway, 2003; Zhang et al., 1999). We did not observe an effect of adrenergic antagonists on DA-mediated depression in our study, arguing against involvement of ARs. In addition, DA has been shown to activate 5-HT1A, 5-HT2A, 5-HT2C, and 5-HT3 receptors, although with lower potency and efficacy than 5-HT (Bhattacharyya et al., 2006; Oz et al., 2003; Woodward et al., 1992). At the 5-HT2A receptor, DA exhibits biased signaling compared with 5-HT, suggesting the possibility of distinctive signaling profiles (Soman et al., 2020). To our knowledge, a direct determination of the affinity or efficacy of DA at mouse 5-HT1BRs remains to be done.

Limitations of the study

The involvement of 5-HT1BRs in DA-mediated suppression of lateral inhibition is shown here with exogenously applied DA and with endogenously released DA in the presence of cocaine. It remains to be determined where 5-HT1B receptors could be activated in the absence of transporter blockers. Other studies that manipulated DA transporter activity *in vivo* also provided evidence of physiological involvement of 5-HT receptors in the actions of DA in high-DA states (Parson etal., 1996). DA transporter KO mice display hyperactivity, which is attenuated by blocking 5-HT1BRs pharmacologically and with partial KO (Hall et al., 2014). Last, overexpression of 5-HT1BRs in NAc neurons increases locomotor sensitivity to cocaine and alters drug-seeking behavior (Furay et al., 2011; Hoplight et al., 2006; Nair et al., 2013; Neumaier et al., 2002; Pentkowski et al., 2012). It has been hypothesized that 5-HT1BRs act at MSN terminals in the VTA to promote cocaine locomotion. However, given our findings, we propose that 5-HT1BR overexpression may, in part, increase cocaine locomotion by enhancing suppression of lateral inhibition from D2-MSNs in the NAc, as shown by Dobbs etal. (2016).

Final conclusions

Our results add to the existing literature on cross-talk among monoamines and their receptors. Our findings also provide some of the strongest evidence that, in the mouse brain, DA can activate 5-HT1BRs to control synaptic transmission and, consequently, the degree of lateral inhibition among NAc neurons. Because the NAc receives dense DA innervation, whether this receptor cross-talk occurs at other synapses or in other brain regions needs to be explored in future studies. We show that DA has acute actions on NAc lateral inhibition that are pathway specific and that depression at synapses from indirect pathway D2-MSNs requires activation of presynaptic DA D2Rs and 5-HT1BRs, both likely expressed on presynaptic terminals of D2-MSNs.

STAR★METHODS

RESOURCE AVAILABILITY

Lead contact—Further information and requests for resources and reagents should be directed to and will be fulfilled by the lead contact, Dr. Veronica Alvarez (alvarezva@mail.nih.gov).

Materials availability—This study did not generate new unique reagents.

Data and code availability

- Data reported in this paper will be shared upon request to the Lead contact.
- This paper does not report original code.
- Any additional information required to reanalyze the data reported in this paper is available from the lead contact upon request.

EXPERIMENTAL MODEL AND SUBJECT DETAILS

Animals—All experiments and procedures were approved by and performed in accordance with guidelines from NIAAA Animal Care and Use Committee. Adult male and female mice (median age = 10 weeks at surgery; 18 weeks at recordings) were used. Though small sample sizes precluded a rigorous test of sex differences, no obvious differences were observed, and data from male and female mice were pooled. To target MSN subpopulations for optogenetic expression, hemizygous Adora2a-Cre mice (B6.FVB(Cg)-Tg(*Adora2a-Cre*)KG139Gsat/Mmucd, GENSAT 036158-UCD) or Drd1-Cre mice ((B6.FVB(Cg)-Tg(Drd1-Cre) EY262Gsat/Mmucd GENSAT 30989-UCD) were used to target D2-MSNs or D1-MSNs, respectively (Gerfen et al., 2013; Gong et al., 2007). For the vast majority of experiments with Adora2a-Cre or Drd1-Cre mice, they were crossed with Drd1-tdTomato mice (B6.Cg-Tg(Drd1a-tdTomato)6Calak/J, JAX 016204 (Ade et al., 2011) to yield Adora2a-Cre;Drd1-tdTomato or Drd1-Cre;Drd1-tdTomato mice. To generate mice lacking the D_2 receptor in D2-MSNs (iMSN-Drd2 KO mice) $Drd2^{loxp/loxp}$ mice (B6.129S4(FVB)-$Drd2^{tm\ 1.1Mrub}$/J JAX 020631) were crossed with Adora2a-Cre mice or Adora2a-Cre;Drd1-tdTomato mice (Lemos et al., 2016). To simultaneously restrict viral mediated expression of ChR2 to D2-MSNs and ChrimsonR to midbrain dopamine neurons, hemizygous Adora2a-Cre mice were crossed with heterozygous DAT-Cre mice (B6.SJL-$Slc6a3^{tm1.1(cre)Bkmn}$/J mice, JAX 006660) (Bäckman et al., 2006) to yield Adora2a-Cre;DAT-Cre mice. 5-HT1B receptor knockout mice (5-HT1BKO) (Ramboz et al., 1995) were maintained on a BALB/c background (C.129-$Htr1b^{tm1Rhn}$/MpenJ) (provided by Dr. John Williams, Vollum Institute; currently JAX 029609) and crossed with Adora2a-Cre;Drd1-tdTomato mice to generate 5-HT1BKO; Adora2a-Cre;Drd1-tdTomato mice on a mixed BALB/c/C57Bl6 background. All other mice in this study were maintained on a C57Bl6 background. Animals were group housed in 12-h light/dark cycle with food and water *ad libitum*. Brain slices were prepared during the light cycle (ZT4.5 ± 2).

METHODS DETAILS

Viral vector injections—Mice (>5 weeks, median = 10 weeks at surgery) were anesthetized with isoflurane (5% induction, ~2% throughout surgery) and placed in the stereotaxic device (Kopf Instruments). Adeno-associated viral (AAV) vectors were injected through a small glass pipette with a Nanoject II (Drummond Scientific) at a rate of ~130 nL/min. Injection pipette was kept in place 5-10 min to allow diffusion, then slowly retracted over the course of 5 min to prevent backflow up the injection tract. To target ChR2 to D2- or D1- MSNs, a Cre-dependent vector encoding ChR2-eYFP (AAV5-EF1a-double floxed-hChR2(H134R)-EYFP-WPRE-HGHpA, 1×10^{13} vg/mL, Addgene# 20298-AAV5 or

AAV5-EF1a-DIO-hChR2(H134R)-EYFP, 4.5 × 10^{12} vg/mL, UNC Vector Core catalog# 5EF1aChR2YFPDIO) was injected bilaterally into NAc core (250–300 nL/side; from bregma: AP, +1.2; ML, ±1.0; DV, −4.8 mm) of Adora2a-Cre or Drd1-Cre mice. For dual D2-MSN/dopamine neuron stimulation experiments Adora2a-Cre;DAT-Cre mice were injected with Cre-dependent ChR2-eYFP in the NAc core (as above), as well as with Cre-dependent virus encoding ChrimsonR-tdTomato (AAV5-Syn-FLEX-rc [ChrimsonR-tdTomato], 5 × 10^{12} vg/mL Addgene # 62723-AAV5) bilaterally into the ventral tegmental area (VTA) (350–500 nL/side; from bregma: AP, −3.1; ML, ±0.5; DV, −4.5 mm) for a total of four injection sites. Recordings were performed at least 2 weeks (6 for ChR2+ChrimsonR injected animals) after surgery to allow time for adequate expression. Prior to recording, viral expression in slices was confirmed by fluorescence visualization.

Slice preparation—Mice were anesthetized with isoflurane and transcardially perfused with 95%O_2/5%CO_2 oxygenated, ice-cold “cutting solution” (in mM: 225 sucrose, 119 NaCl, 2.5 KCl, 0.1 $CaCl_2$, 4.9 $MgCl_2$, 26.2 $NaHCO_3$, 1 NaH_2PO_4, 1.25 glucose, and 3 kynurenic acid). Brains were removed, and sagittal slices (230 μm) were prepared with a vibratome (Leica VT1200) in ice-cold cutting solution (same as perfusion). After slicing, slices were transferred to a holding chamber containing 95%O_2/5%CO_2 oxygenated artificial cerebrospinal fluid (ACSF) (in mM: 124 NaCl, 2.5 KCl, 2.5 $CaCl_2$, 1.3 $MgCl_2$, 26.2 $NaHCO_3$, 1 NaH_2PO_4, 20 glucose, and 0.4 ascorbate) and incubated at 33–34°C for at least 30 min. After incubation, slices were moved to room temperature (22°C–24°C) and covered to minimize light exposure until recording.

Electrophysiology—For recording, slices were transferred to the recording chamber mounted on an upright microscope (BX51WI, Olympus, USA) and perfused (~2 mL/min) with oxygenated ACSF (same as holding chamber) maintained at 31 ± 1°C. Cells were visualized with a 40x (0.8 NA) water-immersion objective illuminated with differential interference contrast. Whole-cell recordings were performed from MSNs in NAc core (generally below the anterior commissure along the whole rostral-caudal axis, from sagittal slices roughly corresponding to 0.8–1.45 mm lateral from bregma) with glass electrodes (2.0–4.0 MΩ) filled with a mixed CsCl/CsMeSO4 based internal solution (in mM: 60 CsCl, 60 CsMeSO4, 10 HEPES, 0.2 EGTA, 4 Na-ATP, 0.4 Na-GTP, 10 phosphocreatine, and 4.4 QX-314 pH = 7.3, ~310 mOsm). Cells were voltage clamped at −55 mV and data were collected using a Multiclamp 700B amplifier low-pass filtered at 2 kHz and digitized at 20 kHz using pClamp v10.3 software (Molecular Devices). Access resistance was monitored throughout experiments, and cells were removed from analysis if it changed >15% from baseline period.

For optogenetic stimulation of ChR2 alone, a fiber optic (200 μm/0.22 NA) connected to a diode-pumped blue laser (473 nm; 25 mW; CrystaLaser) delivered single or paired pulse (50ms interval) stimulation (0.1–0.5 ms; ~0.2 mW) every 20 s to evoke optogenetic inhibitory post synaptic currents (oIPSCs).

After whole-cell break in, cells were given at least 10 min to dialyze internal solution before baseline recording began. For antagonist pretreatment experiments, antagonist was applied at least 3 min before beginning of baseline period. All experiments except those in Figures 2,

S2, S3, 7C, and 7D (DA axon stimulation) were performed in the presence of NBQX (5 μM) and CPP (5 μM) to block AMPA and NMDA receptors, respectively.

Dual ChrimsonR and ChR2 optogenetic stimulation—For dual ChR2 and ChrimsonR stimulation experiments, a 405 nm fiber coupled LED (Thor M405FP1) was used to stimulate ChR2 evoked oIPSCs every 20 s. Pulse width was kept at 0.5 ms and power level was kept below 1.4 mW to minimize possible activation of ChrimsonR (Figure S2F). ChrimsonR stimulation was delivered through the 40x objective centered on the patched cell from a high-powered white LED (Thor Solis1C) through a 620 nm excitation filter (Chroma ET620/60x). ChrimsonR stimulation was delivered as a 20 hz train of 10 pulses (5 ms pulse width, 1.45 mW power measured at objective tip) beginning 1 s before ChR2 stimulation.

Cell identification—MSNs were identified based on size, lack of spontaneous activity, and low membrane resistance at whole cell break-in. D1-MSNs were identified visually by the presence of tdTomato and/or electrophysiologically by the presence of a ChR2 current in ChR2 transduced Drd1-Cre animals. D2-MSNs were identified by MSN characteristics combined with lack of Drd1-tdtomato fluorescence and/or the presence of a ChR2 current in ChR2 transduced Adora2a-Cre animals (putative D2-MSNs).

When recording from and stimulating the same population with possible ChR2 expression (i.e., D2-MSN→D2-MSN synapses) ChR2 currents were identified by their quick onset compared to synaptic currents (<1ms from light on). In these recordings, the stimulation fiber optic was moved around the slice to minimize the amplitude ratio of the ChR2 current to the synaptic current. If unsuccessful, the cell was discarded. At the end of experiments with a ChR2 current, a GABA-A antagonist (gabazine 5 μM) was added to the bath that already contained AMPA and NMDA antagonists to block all fast synaptic transmission and isolate the ChR2 current. During analysis, an average of ~10 sweeps of isolated ChR2 current was subtracted from each trace in the recording to isolate the synaptic current (Figure S1A). All analysis reported was performed on the isolated synaptic current.

Fast-scan cyclic voltammetry—FSCV was performed in NAc core from Adora2a-Cre;DAT-Cre mice virally transduced with Cre-dependent ChrimsonR in midbrain DA neurons in separate slices from those used to record D2-MSN GABA. Carbon-fiber electrodes (CFEs) were prepared with a cylindrical carbon-fiber (7 μm diameter, ~150 μm of exposed fiber) inserted into a glass pipette. Before use, the CFEs were conditioned with an 8-ms-long triangular voltage ramp (−0.4 to 1.2 and back to −0.4 V vs Ag/AgCl reference at 400 V/s) delivered every 15 ms. CFEs showing current >1.8 μA or <1.0 μA in response to the voltage ramp at ~0.6 V were discarded. During the recording, the CFEs were held at μ0.4 V versus Ag/AgCl, and the same triangular voltage ramp was delivered every 100 ms. DA transients were evoked by optical single pulse, or 10 pulses at 20 Hz stimulations using either 590 nm LED or 405 nm LED light through a fiber-optic (200 μm diameter, 0.22 NA, ThorLabs). Data were collected using a Chem-Clamp amplifier (Dagan Corporation) low-pass filtered at 3 kHz and digitized at 100 kHz using an I/O board (National Instruments) with a custom written software VIGOR using Igor Pro (Wavemetrics) running mafPC (courtesy of M.A. Xu-Friedman). The current peak amplitudes of the evoked

DA transients were converted to DA concentration according to the post experimental calibration using 1 μM DA.

Drugs—Dopamine solutions were made fresh daily and kept covered in aluminum foil and on ice to minimize oxidation. All other agonist and antagonists were prepared as stock solutions (1:1000-1:10,000) in DI water or dimethylsulfoxide (DMSO) and diluted into ACSF prior to experiments. The bath concentration of Rubi-GABA perfusion was 10 μM. Cocaine HCl was obtained from the National Institute on Drug Abuse. Dopamine, NEM, kynurenic acid, and methysergide were obtained from Sigma. CPP, gabazine, SCH-23390, yohimbine, citalopram, and GR 127935 were obtained from Abcam. CGP 55845 was obtained from Hello Bio Inc. NBQX was obtained from Hello Bio Inc. and Abcam. Kynurenic acid was obtained from Hello Bio and Sigma. All other drugs were obtained from Tocris.

QUANTIFICATION AND STATISTICAL ANALYSIS

All plots displaying oIPSC amplitude time courses show averages of 3 sweeps per 1 min or 6 sweeps every 2 min, except in Figure 2E, which shows individual sweeps. Before averaging recordings, amplitudes were normalized to mean amplitude during baseline, defined as the 5–10 min period preceding drug application or DA neuron stimulation. For data in which drugs were bath applied, representative traces displayed are the average of the last 6 consecutive traces (2 min recording) of baseline and of drug application periods for a single cell. For endogenously stimulated dopamine release (Figure 2D), representative traces are averages of 6 nonconsecutive traces immediately preceding the dopamine neuron stimulation and 6 traces immediately following dopamine neuron stimulation from a single cell. Dopamine transients presented (Figures 2B and S2A) are average of 5–10 transients from a single recording.

oIPSC amplitude summary bar graphs represent average normalized oIPSC amplitude during the last 3–5 min of baseline period and drug wash. Coefficient of variation was calculated as (standard deviation/mean) * 100% during the same time periods as amplitude summary bar graphs. Electrophysiology data were analyzed using a combination of Clampfit (Molecular Devices), Excel (Microsoft), and Prism (Graphpad). FSCV data were analyzed using Igor Pro.

Statistical analyses were done using one way (ANOVA) and two-way repeated measures ANOVAs (2W RM ANOVA), and paired and unpaired t-tests, where appropriate, for IPSC amplitude comparisons, and Wilcoxon matched-pairs signed rank tests were used for for comparisons of CV and PPR data. Tests performed are reported in the figure legends and text. N's reported represent individual cells/slices. Full statistical test information and animal numbers are presented in Table S1. Time course data are presented as mean ± SEM. Bar graphs are presented as mean ± SEM and/or individual data points. Results were considered significant at an alpha of 0.05. * denotes $p < 0.05$, **$p < 0.01$, ***$p < 0.001$, ****$p < 0.0001$; ns (non-significant) denotes $p > 0.05$.

Supplementary Material

Refer to Web version on PubMed Central for supplementary material.

ACKNOWLEDGMENTS

This study was funded by NIH-IRP (ZIA-AA000421). We thank Dr. David Lovinger and Alvarez lab members for helpful discussions, Roland Bock for sharing FSCV Igor procedures, Dr. J.T. Williams (OHSU) for 5-HT1B knockout, and Drs. Deisseroth and Boyden for ChR2 and ChrimsonR constructs.

REFERENCES

Ade KK, Wan Y, Chen M, Gloss B, and Calakos N (2011). An improved BAC transgenic fluorescent reporter line for sensitive and specific identification of striatonigral medium spiny neurons. Front. Syst. Neurosci 5, 32. 10.3389/fnsys.2011.00032. [PubMed: 21713123]

Adham N, Tamm JA, Salon JA, Vaysse PJJ, Weinshank RL, and Branchek TA (1994). A single point mutation increases the affinity of serotonin 5-HT1Dα, 5-HT1Dβ, 5-HT1E and 5-HT1F receptors for β-adrenergic antagonists. Neuropharmacology 33, 387–391. 10.1016/0028-3908(94)90068-x. [PubMed: 7984276]

Adrover MF, Shin JH, and Alvarez VA (2014). Glutamate and dopamine transmission from midbrain dopamine neurons share similar release properties but are differentially affected by cocaine. J. Neurosci 34, 3183–3192. 10.1523/jneurosci.4958-13.2014. [PubMed: 24573277]

Augustin SM, Chancey JH, and Lovinger DM (2018). Dual dopaminergic regulation of corticostriatal plasticity by cholinergic interneurons and indirect pathway medium spiny neurons. Cell Rep. 24, 2883–2893. 10.1016/j.celrep.2018.08.042. [PubMed: 30208314]

Azmitia EC (2007). Serotonin and brain: evolution, neuroplasticity, and homeostasis. Int. Rev. Neurobiol 77, 31–56. 10.1016/s0074-7742(06)77002-7. [PubMed: 17178471]

Bäckman CM, Malik N, Zhang Y, Shan L, Grinberg A, Hoffer BJ, Westphal H, and Tomac AC (2006). Characterization of a mouse strain expressing Cre recombinase from the 3' untranslated region of the dopamine transporter locus. Genesis 44, 383–390. 10.1002/dvg.20228. [PubMed: 16865686]

Barron AB, Søvik E, and Cornish JL (2010). The roles of dopamine and related compounds in reward-seeking behavior across animal phyla. Front. Behav. Neurosci 4, 1–9. 10.3389/fnbeh.2010.00163. [PubMed: 20126432]

Berke JD (2018). What does dopamine mean? Nat. Neurosci 21, 787–793. 10.1038/s41593-018-0152-y. [PubMed: 29760524]

Berridge KC (2007). The debate over dopamine's role in reward: the case for incentive salience. Psychopharmacology 191, 391–431. 10.1007/s00213-006-0578-x. [PubMed: 17072591]

Bertran-Gonzalez J, Bosch C, Maroteaux M, Matamales M, Hervé D, Valjent E, and Girault J-A (2008). Opposing patterns of signaling activation in dopamine D1 and D2 receptor-expressing striatal neurons in response to cocaine and haloperidol. J. Neurosci 28, 5671–5685. 10.1523/jneurosci.1039-08.2008. [PubMed: 18509028]

Bhattacharyya S, Raote I, Bhattacharya A, Miledi R, and Panicker MM (2006). Activation, internalization, and recycling of the serotonin 2A receptor by dopamine. Proc. Natl. Acad. Sci. U S A 103, 15248–15253. 10.1073/pnas.0606578103. [PubMed: 17005723]

Britt JP, Benaliouad F, McDevitt RA, Stuber GD, Wise RA, and Bonci A (2012). Synaptic and behavioral profile of multiple glutamatergic inputs to the nucleus accumbens. Neuron 76, 790–803. 10.1016/j.neuron.2012.09.040. [PubMed: 23177963]

Bromberg-Martin ES, Matsumoto M, and Hikosaka O (2010). Dopamine in motivational control: rewarding, aversive, and alerting. Neuron 68, 815–834. 10.1016/j.neuron.2010.11.022. [PubMed: 21144997]

Burke DA, Rotstein HG, and Alvarez VA (2017). Striatal local circuitry: a new framework for lateral inhibition. Neuron 96, 267–284. 10.1016/j.neuron.2017.09.019. [PubMed: 29024654]

Chang HT, and Kitai ST (1985). Projection neurons of the nucleus accumbens: an intracellular labeling study. Brain Res. 347, 112–116. 10.1016/0006-8993(85)90894-7. [PubMed: 2996712]

Coddington LT, and Dudman JT (2019). Learning from action: reconsidering movement signaling in midbrain dopamine neuron activity. Neuron 104, 63–77. 10.1016/j.neuron.2019.08.036. [PubMed: 31600516]

Conductier G, Nahon JL, and Guyon A (2011). Dopamine depresses melanin concentrating hormone neuronal activity through multiple effects on α2-noradrenergic, D1 and D2-like dopaminergic receptors. Neuroscience 178, 89–100. 10.1016/j.neuroscience.2011.01.030. [PubMed: 21262322]

Corkrum M, Martin ED, Thomas MJ, Kofuji P, Araque A, Covelo A, Lines J, Bellocchio L, Pisansky M, Loke K, et al. (2020). Dopamine-evoked synaptic regulation in the nucleus accumbens requires astrocyte a. Neuron 105, 1036–1047.e5. 10.1016/j.neuron.2019.12.026. [PubMed: 31954621]

Cornil CA, and Ball GF (2008). Interplay among catecholamine systems: dopamine binds to alpha 2-adrenergic receptors in birds and mammals. J. Comp. Neurol 511, 610–627. 10.1002/cne.21861. [PubMed: 18924139]

Cornil CA, Castelino CB, and Ball GF (2008). Dopamine binds to α2-adrenergic receptors in the song control system of zebra finches (Taeniopygia guttata). J. Chem. Neuroanat 35, 202–215. 10.1016/j.jchem-neu.2007.10.004. [PubMed: 18155403]

Le Crom S, Kapsimali M, Barôme PO, and Vernier P (2003). Dopamine receptors for every species: gene duplications and functional diversification in Craniates. J. Struct. Funct. Genomics 3, 161–176. 10.1007/978-94-010-0263-9_16. [PubMed: 12836695]

Czubayko U, and Plenz D (2002). Fast synaptic transmission between striatal spiny projection neurons. Proc. Natl. Acad. Sci. U S A 99, 15764–15769. 10.1073/pnas.242428599. [PubMed: 12438690]

Dobbs LK, Kaplan AR, Lemos JC, Matsui A, Rubinstein M, and Alvarez VA (2016). Dopamine regulation of lateral inhibition between striatal neurons gates the stimulant actions of cocaine. Neuron 90, 1100–1113. 10.1016/j.neuron.2016.04.031. [PubMed: 27181061]

Dölen G, Darvishzadeh A, Huang KW, and Malenka RC (2013). Social reward requires coordinated activity of nucleus accumbens oxytocin and serotonin. Nature 501, 179–184. 10.1038/nature12518. [PubMed: 24025838]

Floresco SB (2015). The nucleus accumbens: an interface between cognition, emotion, and. Annu. Rev. Psychol 66, 25–52. 10.1146/an-nurev-psych-010213-115159. [PubMed: 25251489]

Francis TC, Yano H, Demarest TG, Shen H, and Bonci A (2019). High-frequency activation of nucleus accumbens D1-MSNs drives excitatory potentiation on D2-MSNs. Neuron 103, 432–444.e3. 10.1016/j.neuron.2019.05.031. [PubMed: 31221559]

Furay AR, Neumaier JF, Mullenix AT, Kaiyala KK, Sandygren NK, and Hoplight BJ (2011). Overexpression of 5-HT1B mRNA in nucleus accumbens shell projection neurons differentially affects microarchitecture of initiation and maintenance of ethanol consumption. Alcohol 45, 19–32. 10.1016/j.alcohol.2010.07.010. [PubMed: 20843634]

Gangarossa G, Espallergues J, d'Exaerde A, de K, El Mestikawy S, Gerfen CR, Hervé D, Girault JA, and Valjent E (2013). Distribution and compartmental organization of GABAergic medium-sized spiny neurons in the mouse nucleus accumbens. Front. Neural Circuits 7, 1–20. 10.3389/fncir.2013.00022. [PubMed: 23440175]

Gerfen CR, Paletzki R, and Worley P (2008). Differences between dorsal and ventral striatum in Drd1a dopamine receptor coupling of dopamine- and cAMP-regulated phosphoprotein-32 to activation of extracellular signal-regulated kinase. J. Neurosci 28, 7113–7120. 10.1523/jneurosci.3952-07.2008. [PubMed: 18614680]

Gerfen CR, Paletzki R, and Heintz N (2013). GENSAT BAC cre-recombinase driver lines to study the functional organization of cerebral cortical and basal ganglia circuits. Neuron 80, 1368–1383. 10.1016/j.neuron.2013.10.016. [PubMed: 24360541]

Gong S, Doughty M, Harbaugh CR, Cummins A, Hatten ME, Heintz N, and Gerfen CR (2007). Targeting Cre recombinase to specific neuron populations with bacterial artificial chromosome constructs. J. Neurosci 27, 9817–9823. 10.1523/jneurosci.2707-07.2007. [PubMed: 17855595]

Goto Y, and Grace AA (2005). Dopamine-dependent interactions between limbic and prefrontal cortical plasticity in the nucleus accumbens: disruption by cocaine sensitization. Neuron 47, 255–266. 10.1016/j.neuron.2005.06.017. [PubMed: 16039567]

Guiard BP, El Mansari M, and Blier P (2008). Cross-talk between dopaminergic and noradrenergic systems in the rat ventral tegmental area, locus ceruleus, and dorsal hippocampus. Mol. Pharmacol 74, 1463–1475. 10.1124/mol.108.048033. [PubMed: 18703671]

Guzmán JN, Hernández A, Galarraga E, Tapia D, Laville A, Vergara R, Aceves J, and Bargas J (2003). Dopaminergic modulation of axon collaterals interconnecting spiny neurons of the rat striatum. J. Neurosci 23, 8931–8940. 10.1523/jneurosci.23-26-08931.2003. [PubMed: 14523095]

Hall FS, Sora I, Hen R, and Uhl GR (2014). Serotonin/dopamine interactions in a hyperactive mouse: reduced serotonin receptor 1B activity reverses effects of dopamine transporter knockout. PLoS One 9, e115009–20. 10.1371/journal.pone.0115009. [PubMed: 25514162]

Hamid AA, Pettibone JR, Mabrouk OS, Hetrick VL, Schmidt R, Vander Weele CM, Kennedy RT, Aragona BJ, and Berke JD (2015). Mesolimbic dopamine signals the value of work. Nat. Neurosci 19, 117–126. 10.1038/nn.4173. [PubMed: 26595651]

Hjelmstad GO (2004). Dopamine excites nucleus accumbens neurons through the differential modulation of glutamate and GABA release. J. Neurosci 24, 8621–8628. 10.1523/jneurosci.3280-04.2004. [PubMed: 15456835]

Hoplight BJ, Sandygren NA, and Neumaier JF (2006). Increased expression of 5-HT1B receptors in rat nucleus accumbens via virally mediated gene transfer increases voluntary alcohol consumption. Alcohol 38, 73–79. 10.1016/j.alcohol.2006.04.003. [PubMed: 16839853]

Hoyer D (1988). Functional correlates of serotonin 5-HT1 recognition sites. J. Receptors Signal Transduction 8, 59–81. 10.3109/10799898809048978.

Ikemoto S, and Panksepp J (1999). The role of nucleus accumbens dopamine in motivated behavior: a unifying interpretation with special reference to reward-seeking. Brain Res. Rev 31, 6–41. 10.1016/s0165-0173(99)00023-5. [PubMed: 10611493]

de Jong JW, Afjei SA, Pollak Dorocic I, Peck JR, Liu C, Kim CK, Tian L, Deisseroth K, and Lammel S (2019). A neural circuit mechanism for encoding aversive Stimuli in the mesolimbic dopamine system. Neuron 101, 133–151.e7. 10.1016/j.neuron.2018.11.005. [PubMed: 30503173]

Kim HR, Uchida N, Malik AN, Mikhael JG, Bech P, Tsutsui-Kimura I, Sun F, Zhang Y, Li Y, Watabe-Uchida M, et al. (2020).A unified framework for dopamine signals across timescales. Cell 183, 1600–1616.e25. 10.1016/j.cell.2020.11.013. [PubMed: 33248024]

Kohnomi S, Koshikawa N, and Kobayashi M (2012). D(2)-like dopamine receptors differentially regulate unitary IPSCs depending on presynaptic GABAergic neuron subtypes in rat nucleus accumbens shell. J. Neurophysiol 107, 692–703. 10.1152/jn.00281.2011. [PubMed: 22049335]

Kohnomi S, Ebihara K, and Kobayashi M (2017). Suppressive regulation of lateral inhibition between medium spiny neurons via dopamine D1 receptors in the rat nucleus accumbens shell. Neurosci. Lett 636, 58–63. 10.1016/j.neulet.2016.10.049. [PubMed: 27793700]

Kourrich S, and Thomas MJ (2009). Similar neurons, opposite adaptations: psychostimulant experience differentially alters firing properties in accumbens core versus shell. J. Neurosci 29, 12275–12283. 10.1523/jneurosci.3028-09.2009. [PubMed: 19793986]

Lahiri AK, and Bevan MD (2020). Dopaminergic transmission rapidly and persistently enhances excitability of D1 receptor-expressing striatal projection neurons. Neuron 106, 277–290.e6. 10.1016/j.neuron.2020.01.028. [PubMed: 32075716]

Lanau F, Zenner MT, Civelli O, and Hartman DS (2002). Epinephrine and norepinephrine act as potent agonists at the recombinant human dopamine D4 receptor. J. Neurochem 68, 804–812. 10.1046/j.1471-4159.1997.68020804.x.

Larsen MB, Sonders MS, Mortensen OV, Larson GA, Zahniser NR, and Amara SG (2011). Dopamine transport by the serotonin transporter: a Mechanistically distinct mode of substrate translocation. J. Neurosci 31, 6605–6615. 10.1523/jneurosci.0576-11.2011. [PubMed: 21525301]

Lee K, Claar LD, Hachisuka A, Bakhurin KI, Nguyen J, Trott JM, Gill JL, and Masmanidis SC (2020). Temporally restricted dopaminergic control of reward-conditioned movements. Nat. Neurosci 23, 209–216. 10.1038/s41593-019-0567-0. [PubMed: 31932769]

Lemos JC, Friend DM, Kaplan AR, Shin JH, Rubinstein M, Kravitz AV, and Alvarez VA (2016). Enhanced GABA transmission drives bradykinesia following loss of dopamine D2 receptor signaling. Neuron 90, 824–838. 10.1016/j.neuron.2016.04.040. [PubMed: 27196975]

Lloyd K, and Dayan P (2015). Tamping ramping: algorithmic, Implementational, and computational explanations of phasic dopamine signals in the accumbens. PLoS Comput. Biol 11, e1004622, 34. 10.1371/jour-nal.pcbi.1004622. [PubMed: 26699940]

Marcott PF, Mamaligas AA, and Ford CP (2014). Phasic dopamine release drives rapid activation of striatal D2-receptors. Neuron 84, 164–176. 10.1016/j.neuron.2014.08.058. [PubMed: 25242218]

Marcott PF, Gong S, Donthamsetti P, Grinnell SG, Nelson MN, Newman AH, Birnbaumer L, Martemyanov KA, Javitch JA, and Ford CP (2018). Regional heterogeneity of D2-receptor signaling in the dorsal striatum and nucleus accumbens. Neuron 98, 575–587.e4. 10.1016/j.neuron.2018.03.038. [PubMed: 29656874]

Markstein R, Hoyer D, and Engel G (1986). 5-HT1A-receptors mediate stimulation of adenylate cyclase in rat hippocampus. Naunyn-Schmiedeberg's Arch. Pharmacol 333, 335–341. 10.1007/bf00500006. [PubMed: 2945992]

Maroteaux L, Saudou F, Amlaiky N, Boschert U, Plassat JL, and Hen R (1992). Mouse 5HT1B serotonin receptor: cloning, functional expression, and localization in motor control centers. Proc. Natl. Acad. Sci. U S A 89, 3020–3024. 10.1073/pnas.89.7.3020. [PubMed: 1557407]

Matamales M, McGovern AE, Mi JD, Mazzone SB, Balleine BW, and Bertran-Gonzalez J (2020). Local D2- to D1-neuron transmodulation updates goal-directed learning in the striatum. Science 367, 549–555. 10.1126/science.aaz5751. [PubMed: 32001651]

Mathur BN, Capik NA, Alvarez VA, and Lovinger DM (2011). Serotonin induces long-term depression at corticostriatal synapses. J. Neurosci 31, 7402–7411. 10.1523/jneurosci.6250-10.2011. [PubMed: 21593324]

Matsui A, and Alvarez VA (2018). Cocaine inhibition of synaptic transmission in the ventral pallidum is pathway-specific and mediated by serotonin. Cell Rep. 23, 3852–3863. 10.1016/j.celrep.2018.05.076. [PubMed: 29949769]

McCorvy JD, and Roth BL (2015). Structure and function of serotonin G protein-coupled receptors. Pharmacol. Ther 150, 129–142. 10.1016/j.pharmthera.2015.01.009. [PubMed: 25601315]

Metcalf MA, McGuffin RW, and Hamblin MW (1992). Conversion of the human 5-HT1Dβ serotonin receptor to the rat 5-HT1b ligand-binding phenotype by Thr355 ASN site directed mutagenesis. Biochem. Pharmacol 44, 1917–1920. 10.1016/0006-2952(92)90092-w. [PubMed: 1449511]

Millan MJ, Newman-Tancredi A, Quentric Y, and Cussac D (2001). The "selective" dopamine D1 receptor antagonist, SCH23390, is a potent and high efficacy agonist at cloned human serotonin2C receptors. Psychopharmacology 156, 58–62. 10.1007/s002130100742. [PubMed: 11465634]

Mogenson GJ, Jones DL, and Yim CY (1980). From motivation to action: functional interface between the limbic system and the motor system. Prog. Neurobiol 14, 69–97. 10.1016/0301-0082(80)90018-0. [PubMed: 6999537]

Morón JA, Brockington A, Wise RA, Rocha BA, and Hope BT (2002). Dopamine uptake through the norepinephrine transporter in brain regions with low levels of the dopamine transporter: evidence from knock-out mouse lines. J. Neurosci 22, 389–395. 10.1523/jneurosci.22-02-00389.2002. [PubMed: 11784783]

Nair SG, Furay AR, Liu Y, and Neumaier JF (2013). Differential effect of viral overexpression of nucleus accumbens shell 5-HT1B receptors on stress-and cocaine priming-induced reinstatement of cocaine seeking. Pharmacol. Biochem. Behav 112, 89–95. 10.1016/j.pbb.2013.09.009. [PubMed: 24075973]

Neumaier JF, Vincow ES, Arvanitogiannis A, Wise RA, and Carlezon WA (2002). Elevated expression of 5-HT1B receptors in nucleus accumbens efferents sensitizes animals to cocaine. J. Neurosci 22, 10856–10863. 10.1523/jneurosci.22-24-10856.2002. [PubMed: 12486179]

Nicola SM (2007). The nucleus accumbens as part of a basal ganglia action selection circuit. Psychopharmacology 191, 521–550. 10.1007/s00213-006-0510-4. [PubMed: 16983543]

Nicola SM (2010). The flexible approach hypothesis: unification of effort and cue-responding hypotheses for the role of nucleus accumbens dopamine in the activation of reward-seeking behavior. J. Neurosci 30, 16585–16600. 10.1523/jneurosci.3958-10.2010. [PubMed: 21147998]

Nicola SM, and Malenka RC (1997). Dopamine depresses excitatory and inhibitory synaptic transmission by distinct mechanisms in the nucleus accumbens. J. Neurosci 17, 5697–5710. 10.1523/jneurosci.17-15-05697.1997. [PubMed: 9221769]

Oksenberg D, Marsters SA, O'Dowd BF, Jin H, Havlik S, Peroutka SJ, and Ashkenazi A (1992). A single amino-acid difference confers major pharmacological variation between human and rodent 5-HT1B receptors. Nature 360, 161–163. 10.1038/360161a0. [PubMed: 1436092]

Oz M, Zhang L, Rotondo A, Sun H, and Morales M (2003). Direct activation by dopamine of recombinant human 5-HT1A receptors: comparison with human 5-HT2C and 5-HT3 receptors. Synapse 50, 303–313. 10.1002/syn.10273. [PubMed: 14556235]

Parson LH, Weiss F, and Koob GF (1996). Serotonin 1B receptor stimulation enhances dopamine mediated reinforecement. Psychopharmacology 128, 150–160. [PubMed: 8956376]

Patriarchi T, Zhong H, Dombeck D, von Zastrow M, Nimmerjahn A, Gradinaru V, Williams JT, Tian L, Cho JR, Merten K, et al. (2018). Ultrafast neuronal imaging of dopamine dynamics with designed genetically encoded sensors. Science 360. 10.1126/science.aat4422.

Pennartz CM, Dolleman-Van der Weel MJ, Kitai ST, and Lopes da Silva FH (1992). Presynaptic dopamine D1 receptors attenuate excitatory and inhibitory limbic inputs to the shell region of the rat nucleus accumbens studied in vitro. J. Neurophysiol 67, 1325–1334. 10.1152/jn.1992.67.5.1325. [PubMed: 1534574]

Pennartz CM, Groenewegen HJ, and Lopes da Silva FH (1994). The nucleus accumbens as a complex of functionally distinct neuronal ensembles: an integration of behavioural, electrophysiological and anatomical data. Prog. Neurobiol 42, 719–761. 10.1016/0301-0082(94)90025-6. [PubMed: 7938546]

Pentkowski NS, Cheung THC, Toy WA, Adams MD, Neumaier JF, and Neisewander JL (2012). Protracted withdrawal from cocaine self-administration flips the switch on 5-HT1B receptor modulation of cocaine abuse-related behaviors. Biol. Psychiatry 72, 396–404. 10.1016/j.biopsych.2012.03.024. [PubMed: 22541946]

Peroutka SJ, and Snyder SH (1979). Multiple serotonin receptors: differential binding of [3H]5-hydroxytryptamine, [3H]lysergic acid diethylamide and [3H]spiroperidol. Mol. Pharmacol 16, 687–699. [PubMed: 530254]

Planert H, Szydlowski SN, Hjorth JJJ, Grillner S, and Silberberg G (2010). Dynamics of synaptic transmission between fast-spiking interneurons and striatal projection neurons of the direct and indirect pathways. J. Neurosci 30, 3499–3507. 10.1523/jneurosci.5139-09.2010. [PubMed: 20203210]

Pommer S, Akamine Y, Schiffmann SN, de Kerchove d'Exaerde A, and Wickens JR (2021). The effect of serotonin receptor 5-HT1B on lateral inhibition between spiny projection neurons in the mouse striatum. J. Neurosci 41, 7831–7847. 10.1523/jneurosci.1037-20.2021. [PubMed: 34348999]

Puighermanal E, Sanz E, Quintana A, Marsicano G, Martin M, Rubinstein M, Girault JA, Ding JB, Valjent E, Castell L, et al. (2020). Functional and molecular heterogeneity of D2R neurons along dorsal ventral axis in the striatum. Nat. Commun 11, 1957. 10.1038/s41467-020-15716-9. [PubMed: 32327644]

Puryear CB, Kim MJ, and Mizumori SJY (2010). Conjunctive encoding of movement and reward by ventral tegmental area neurons in the freely navigating rodent. Behav. Neurosci 124, 234–247. 10.1037/a0018865. [PubMed: 20364883]

Ramboz S, Saudou F, Amara DA, Belzung C, Segu L, Misslin R, Buhot M-C, and Hen R (1995). 5-HT1 receptor knock out behavioral consequences. Behav. Brain Res 73, 305–312. 10.1016/0166-4328(96)00119-2.

Reynolds JNJ, Hyland BI, and Wickens JR (2001).A cellular mechanism of reward-related learning. Nature 413, 67–70. 10.1038/35092560. [PubMed: 11544526]

Rial Verde EM, Zayat L, Etchenique R, and Yuste R (2008). Photorelease of GABA with visible light using an inorganic caging group. Front. Neural Circuits 2, 1–8. 10.3389/neuro.04.002.2008. [PubMed: 18946541]

Ridray S, Griffon N, Mignon V, Souil E, Carboni S, Diaz J, Schwartz J-C, and Sokoloff P (1998). Coexpression of dopamine D 1 and D 3 receptors in islands of Calleja and shell of nucleus accumbens of the rat: opposite and synergistic functional interactions. Eur. J. Neurosci 10, 1676–1686. 10.1046/j.1460-9568.1998.00173.x. [PubMed: 9751140]

Rodríguez D, Brea J, Loza MI, and Carlsson J (2014). Structure-based Discovery of Selective Serotonin 5-HT(1B) Receptor Ligands. Structure 22, 1140–1151. [PubMed: 25043551]

Roitman MF, Stuber GD, Phillips PEM, Wightman RM, and Carelli RM (2004). Dopamine operates as a subsecond modulator of food seeking. J. Neurosci 24, 1265–1271. 10.1523/jneurosci.3823-03.2004. [PubMed: 14960596]

Root DH, Hoffman AF, Good CH, Zhang S, Gigante E, Lupica CR, and Morales M (2015). Norepinephrine activates dopamine d4 receptors in the rat lateral habenula. J. Neurosci 35, 3460–3469. 10.1523/jneurosci.4525-13.2015. [PubMed: 25716845]

Saddoris MP, Sugam JA, Cacciapaglia F, and Carelli RM (2013). Rapid dopamine dynamics in the accumbens core and shell: learning and action. Front. Biosci. (Elite Edition) E5, E288–E615. 10.2741/e615.

Salamone JD, and Correa M (2012). The mysterious motivational functions of mesolimbic dopamine. Neuron 76, 470–485. 10.1016/j.neuron.2012.10.021. [PubMed: 23141060]

Sánchez-Soto M, Ferre S, Casadó-Anguera V, Yano H, Bender BJ, Cai NS, Moreno E, Canela EI, Cortés A, Meiler J, et al. (2018). α2A- and α2C-adrenoceptors as potential targets for dopamine and dopamine receptor ligands. Mol. Neurobiol 55, 8438–8454. 10.1007/s12035-018-1004-1. [PubMed: 29552726]

Sari Y, Miquel MC, Brisorgueil MJ, Ruiz G, Doucet E, Hamon M, and Verge D (1999). Cellular and subcellular localization of 5-hydroxytryptamine(1B) receptors in the rat central nervous system: Immuno-cytochemical, autoradiographic and lesion studies. Neuroscience 88, 899–915. 10.1016/s0306-4522(98)00256-5. [PubMed: 10363826]

Schoeffter P, and Hoyer D (1989). Interaction of arylpiperazines with 5-HT1A, 5-HT1B, 5-HT1C and 5-HT1D receptors: do discriminatory 5-HT1B receptor ligands exist? Naunyn-Schmiedeberg's Arch. Pharmacol 339, 675–683. 10.1007/bf00168661. [PubMed: 2770889]

Schultz W (2016). Dopamine reward prediction-error signalling: a two-component response. Nat. Rev. Neurosci 17, 183–195. 10.1038/nrn.2015.26. [PubMed: 26865020]

Shapiro MS, Wollmuth LP, and Hille B (1994). Modulation of Ca2+ channels by PTX-sensitive G-proteins is blocked by N-ethylmaleimide in rat sympathetic neurons. J. Neurosci 14, 7109–7116. 10.1523/jneurosci.14-11-07109.1994. [PubMed: 7525895]

Shen HW, Uhl GR, Sora I, Hagino Y, Kobayashi H, Shinohara-Tanaka K, Ikeda K, Yamamoto H, Yamamoto T, Lesch KP, et al. (2004). Regional differences in extracellular dopamine and serotonin assessed by in vivo microdialysis in mice lacking dopamine and/or serotonin transporters. Neuropsychopharmacology 29, 1790–1799. 10.1038/sj.npp.1300476. [PubMed: 15226739]

Shin JH, Adrover MF, and Alvarez VA (2017). Distinctive modulation of dopamine release in the nucleus accumbens shell mediated by dopamine and acetylcholine receptors. J. Neurosci 37, 11166–11180. 10.1523/jneurosci.0596-17.2017. [PubMed: 29030431]

Shindou T, Shindou M, Watanabe S, and Wickens J (2019). A silent eligibility trace enables dopamine-dependent synaptic plasticity for reinforcement learning in the mouse striatum. Eur. J. Neurosci 49, 726–736. 10.1111/ejn.13921. [PubMed: 29603470]

Da Silva JA, Tecuapetla F, Paixão V, and Costa RM (2018). Dopamine neuron activity before action initiation gates and invigorates future movements. Nature 554, 244–248. 10.1038/nature25457. [PubMed: 29420469]

Soman S, Bhattacharya A, and Panicker MM (2020). Dopamine requires unique residues to signal via the serotonin 2A receptor. Neuroscience 439, 319–331. 10.1016/j.neuroscience.2019.03.056. [PubMed: 30970266]

Steinberg EE, Keiflin R, Boivin JR, Witten IB, Deisseroth K, and Janak PH (2013). A causal link between prediction errors, dopamine neurons and learning. Nat. Neurosci 16, 966–973. 10.1038/nn.3413. [PubMed: 23708143]

Stuber GD, Hnasko TS, Britt JP, Edwards RH, and Bonci A (2010). Dopaminergic terminals in the nucleus accumbens but not the dorsal striatum corelease glutamate. J. Neurosci 30, 8229–8233. 10.1523/jneurosci.1754-10.2010. [PubMed: 20554874]

Taverna S, van Dongen YC, Groenewegen HJ, and Pennartz CMA (2004). Direct physiological evidence for synaptic connectivity between medium-sized spiny neurons in rat nucleus accumbens in situ. J. Neurophysiol 91, 1111–1121. 10.1152/jn.00892.2003. [PubMed: 14573550]

Taverna S, Canciani B, and Pennartz CMA (2005). Dopamine D1-receptors modulate lateral inhibition between principal cells of the nucleus accumbens. J. Neurophysiol 93, 1816–1819. 10.1152/jn.00672.2004. [PubMed: 15456801]

Taverna S, Ilijic E, and Surmeier DJ (2008). Recurrent collateral connections of striatal medium spiny neurons are disrupted in models of Parkinson's disease. J. Neurosci 28, 5504–5512. 10.1523/jneurosci.5493-07.2008. [PubMed: 18495884]

Tecuapetla F, Carrillo-Reid L, Bargas J, and Galarraga E (2007). Dopaminergic modulation of short-term synaptic plasticity at striatal inhibitory synapses. Proc. Natl. Acad. Sci. U S A 104, 10258–10263. 10.1073/pnas.0703813104. [PubMed: 17545307]

Tecuapetla F, Koós T, Tepper JM, Kabbani N, and Yeckel MF (2009). Differential dopaminergic modulation of neostriatal synaptic connections of Striatopallidal axon collaterals. J. Neurosci 29, 8977–8990. 10.1523/jneurosci.6145-08.2009. [PubMed: 19605635]

Tecuapetla F, Koos T, Patel JC, Xenias H, English D, Tadros I, Shah F, Berlin J, Deisseroth K, Rice ME, et al. (2010). Glutamatergic signaling by mesolimbic dopamine neurons in the nucleus accumbens. J. Neurosci 30, 7105–7110. 10.1523/jneurosci.0265-10.2010. [PubMed: 20484653]

Tiger M, Varnäs K, Okubo Y, and Lundberg J (2018). The 5-HT 1B receptor - a potential target for antidepressant treatment. Psychopharmacology 235, 1317–1334. 10.1007/s00213-018-4872-1. [PubMed: 29546551]

Tritsch NX, and Sabatini BL (2012). Dopaminergic modulation of synaptic transmission in cortex and striatum. Neuron 76, 33–50. 10.1016/j.neuron.2012.09.023. [PubMed: 23040805]

Tritsch NX, Ding JB, and Sabatini BL (2012). Dopaminergic neurons inhibit striatal output through non-canonical release of GABA. Nature 490, 262–266. 10.1038/nature11466. [PubMed: 23034651]

Tunstall MJ, Oorschot DE, Kean A, and Wickens JR (2002). Inhibitory interactions between spiny projection neurons in the rat striatum. J. Neurophysiol 88, 1263–1269. 10.1152/jn.2002.88.3.1263. [PubMed: 12205147]

Uhlén S, Lindblom J, Tiger G, and Wikberg JES (1997). Quantification of α(2A) and α(2C) adrenoceptors in the rat striatum and in different regions of the spinal cord. Acta Physiol. Scand 160, 407–412. 10.1046/j.1365-201x.1997.00175.x. [PubMed: 9338523]

Virk MS, Sagi Y, Medrihan L, Leung J, Kaplitt MG, and Greengard P (2016). Opposing roles for serotonin in cholinergic neurons of the ventral and dorsal striatum. Proc. Natl. Acad. Sci. U S A 113, 734–739. 10.1073/pnas.1524183113. [PubMed: 26733685]

Wang DV, and Tsien JZ (2011). Conjunctive processing of locomotor signals by the ventral tegmental area neuronal population. PLoS One 6, e16528. 10.1371/journal.pone.0016528. [PubMed: 21304590]

Wei W, Ding S, and Zhou FM (2017). Dopaminergic treatment weakens medium spiny neuron collateral inhibition in the parkinsonian striatum. J. Neurophysiol 117, 987–999. 10.1152/jn.00683.2016. [PubMed: 27927785]

Van Wijngaarden I, Tulp MTM, and Soudijn W (1990). The concept of selectivity in 5-HT receptor research. Eur. J. Pharmacol. Mol. Pharmacol 188, 301–312. 10.1016/0922-4106(90)90190-9.

Woodward RM, Panicker MM, and Miledi R (1992). Actions of dopamine and dopaminergic drugs on cloned serotonin receptors expressed in Xenopus oocytes. Proc. Natl. Acad. Sci. U S A 89, 4708–4712. 10.1073/pnas.89.10.4708. [PubMed: 1350095]

Yagishita S, Hayashi-Takagi A, Ellis-Davies GCR, Urakubo H, Ishii S, and Kasai H (2014).A critical time window for dopamine actions on the structural plasticity of dendritic spines. Science 345, 1616–1620. 10.1126/science.1255514. [PubMed: 25258080]

Yamamoto K, and Vernier P (2011). The evolution of dopamine systems in chordates. Front. Neuroanat 5, 1. 10.3389/fnana.2011.00021. [PubMed: 21373368]

Yang N, Zhang KY, Wang FF, Hu ZA, and Zhang J (2014). Dopamine inhibits neurons from the rat dorsal subcoeruleus nucleus through the activation of α2-adrenergic receptors. Neurosci. Lett 559, 61–66. 10.1016/j.neulet.2013.11.037. [PubMed: 24304869]

Zhang W, and Ordway GA (2003). The α2C-adrenoceptor modulates GABA release in mouse striatum. Mol. Brain Res 112, 24–32. 10.1016/s0169-328x(03)00026-3. [PubMed: 12670699]

Zhang W, Klimek V, Farley JT, Zhu MY, and Ordway GA (1999). al-pha2C adrenoceptors inhibit adenylyl cyclase in mouse striatum: potential activation by dopamine. J. Pharmacol. Exp. Ther 289, 1286–1292. [PubMed: 10336518]

Zhang WP, Ouyang M, and Thomas SA (2004). Potency of catecholamines and other L-tyrosine derivatives at the cloned mouse adrenergic receptors. Neuropharmacology 47, 438–449. 10.1016/j.neuro-pharm.2004.04.017. [PubMed: 15275833]

Highlights

- DA modulation of nucleus accumbens lateral inhibition differs by synapse pair
- Endogenous DA depresses D2-MSN lateral inhibition within 1 s of release
- DA presynaptically depresses D2-MSN transmission through D2 and 5-HT1B receptors

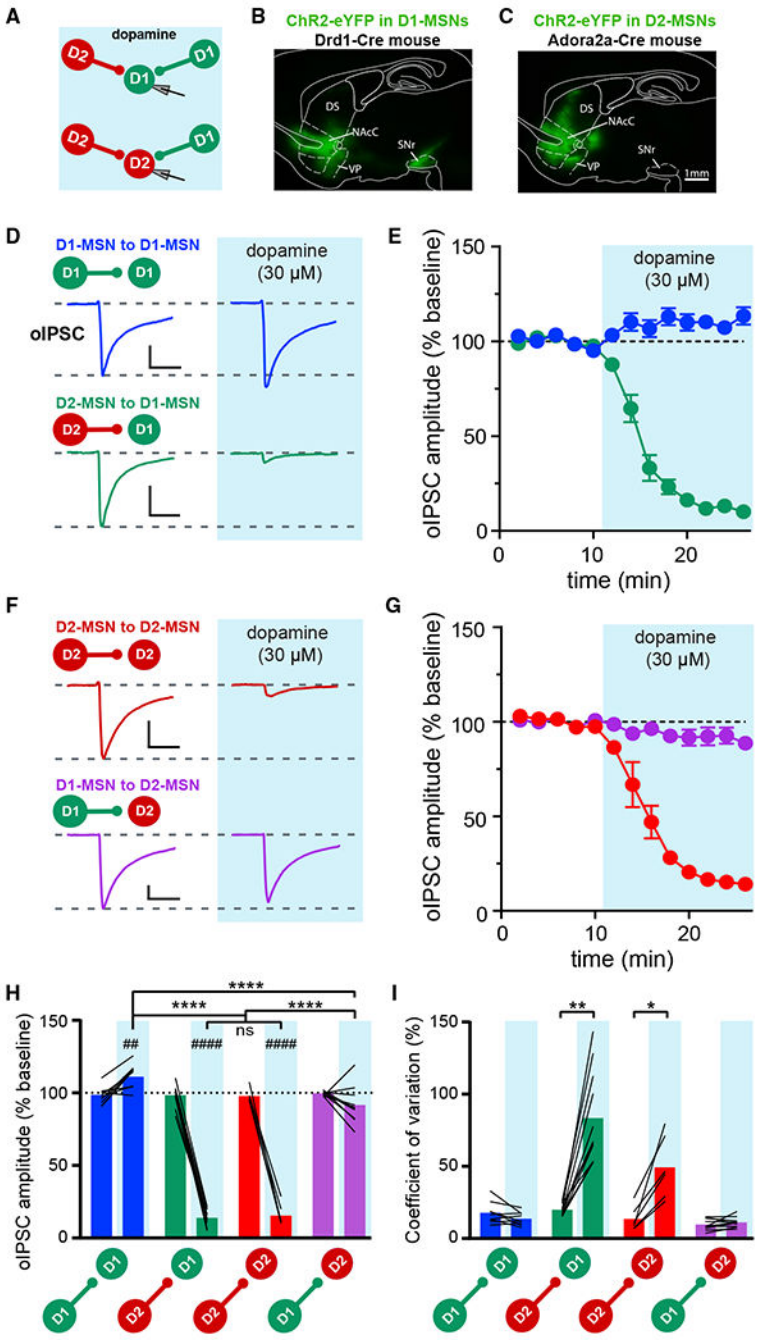

Figure 1. DA depresses D2-MSN lateral inhibition and produces a small potentiation of D1-MSN→D1-MSN lateral inhibition

(A) Diagram showing recordings from D1-MSNs or D2-MSNs while evoking synaptic currents from local MSN axon collaterals expressing ChR2.

(B and C) Sagittal brain slices from (B) Drd1-Cre and (C) Adora2a-Cre mice, showing ChR2-eYFP in D1-MSNs in the NAc core (NAcC) and projections to the midbrain (B) or D2-MSNs and projections to the ventral pallidum (VP). DS, dorsal striatum; SNr, substantia nigra pars reticulata.

(D–F) Representative oIPSC recorded from D1-MSNs (D) or D2-MSNs (F) before and during DA when stimulating D1-MSNs (blue/purple) or D2-MSNs (green/red).
(E–G) Time course of DA effect on normalized oIPSC amplitudes at D1-MSN → D1-MSN (blue) and D2-MSN → D1-MSN (green) synapses (n = 9, 7) (E) or D2-MSN → D2-MSN (red) and D1-MSN → D2-MSN (purple) synapses (n = 6, 10) (G).
(H) Summary of DA effect on D1-MSN → D1-MSN (blue), D2-MSN → D1-MSN (green), D2-MSN → D2-MSN (red), and D1-MSN→D2-MSN (purple) synapses (n = 9, 11, 6, 10). #, significance from baseline; *p < 0.05, Sidak's test following two-way repeated measures (2W RM) ANOVA.
(I) CV of oIPSC amplitude before and during DA (shaded) for D1-MSN → D1-MSN (blue), D2-MSN → D1-MSN (green), D2-MSN → D2-MSN (red), and D1-MSN → D2-MSN (purple) synapses. *p < 0.05 Wilcoxon matched-pairs signed-rank test.
Scale bars: 200 pA, 20 ms. All error bars presented throughout manuscript represent SEM. See full statistics in Table S1.

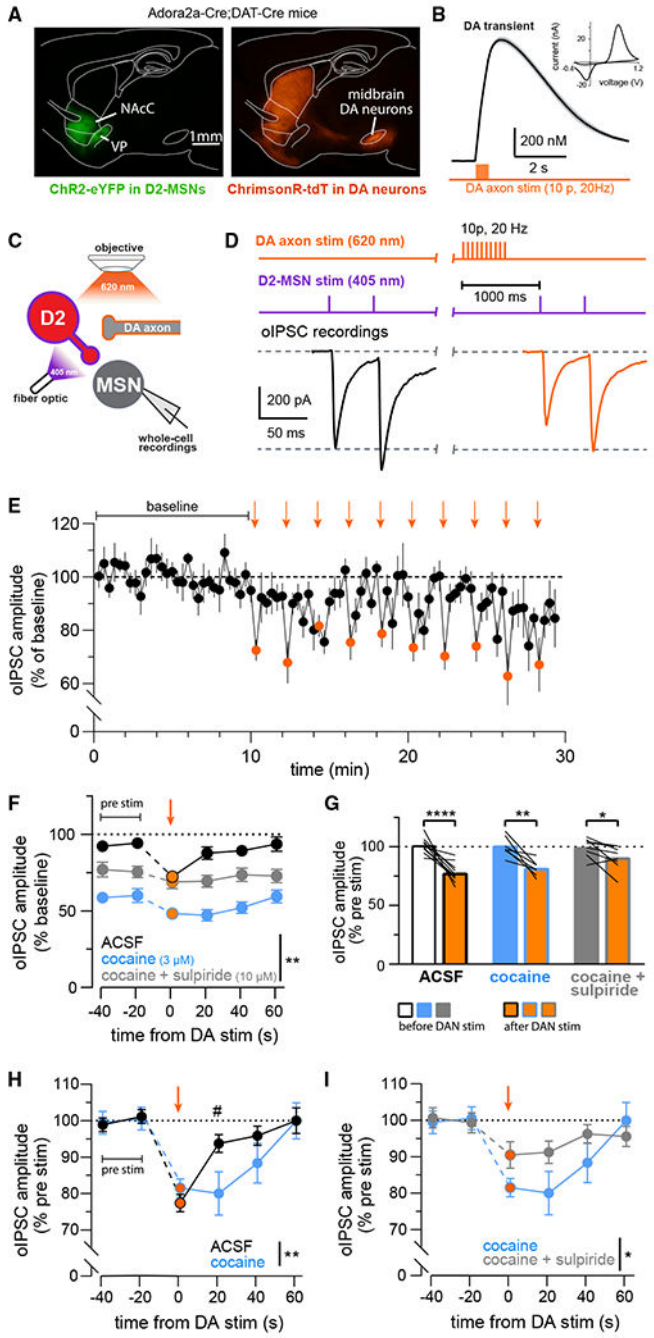

Figure 2. Transient depression of D2-MSN lateral inhibition induced by stimulation of DA neuron axons is prolonged by cocaine and partially blocked by a D2R antagonist

(A) Sagittal brain slice showing, in green, ChR2-eYFP in D2-MSNs with projections to the VP and, in red, ChrimsonR-tdTomato in midbrain DA neurons with projections to the striatum.

(B) DA transients measured with FSCV are evoked by optogenetic stimulation of ChrimsonR. Inset: current-voltage plot showing the characteristic oxidation and reduction peaks for DA.

(C) Dual optogenetic stimulation of DA neuron axons with ChrimsonR to evoke endogenous DA release and D2-MSN with ChR2 to evoke GABA release while recording oIPSCs in MSNs.

(D) Top: the purple line shows the timing of paired pulses of 405-nm light used to activate ChR2, and the orange line shows the timing of a train of 10 pulses of 620-nm light to activate ChrimsonR. Bottom: representative trace before (black) and after (orange) stimulation of DA axons.

(E) Normalized oIPSC amplitudes at D2-MSN → MSN synapses at baseline without stimulation (black) and after (orange) train stimulation of DA axons every 2 min (arrows) (n = 11).

(F) Time course of oIPSC amplitudes before and after DA axon stimulation (8–10 epochs/cell; 11, 7, 8). Orange symbols shows oIPSC preceded by train stimulation of DA axons. *, significant time × drug interaction, 2W RM ANOVA.

(G) Normalized amplitude of oIPSC evoked by D2-MSN stimulation before and after (orange fill) DA axon stimulation in control ACSF (black), cocaine (blue), and cocaine + sulp (gray). Lines show paired data for a single slice. *$p < 0.05$, paired t tests.

(H and I) oIPSC amplitudes before and after DA axon stimulation under each condition, normalized to pre-stimulation (n = 11, 7, 8). *, significant interaction in 2W RM ANOVA (H, time × cocaine; I, time × suip). #$p < 0.05$, Sidak's test.

See full statistics in Table S1.

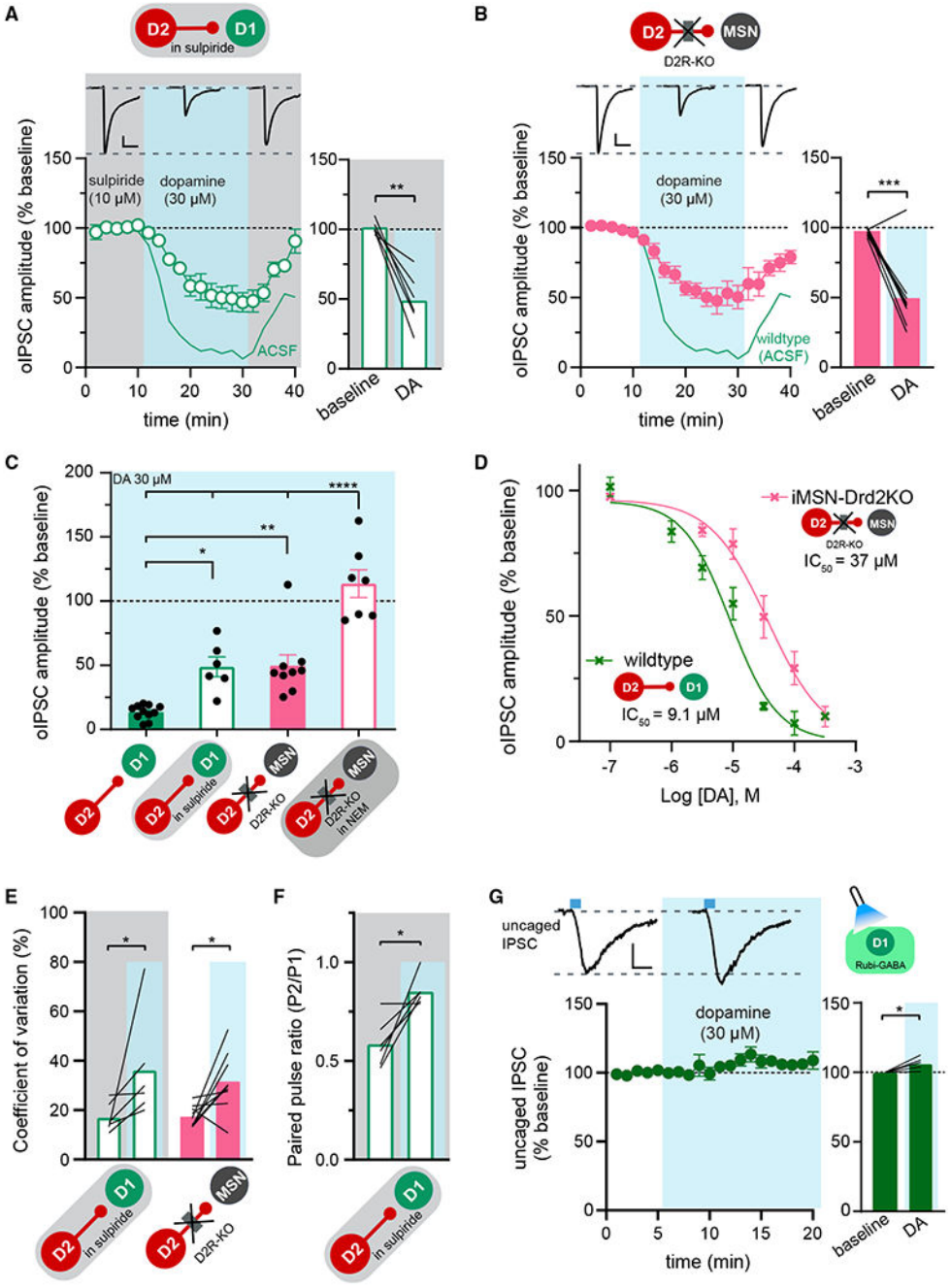

Figure 3. D2R-dependent and -independent mechanisms of presynaptic depression by DA

(A and B) Top: representative traces from D1-MSNs in WT (A) and MSNs in iMSN-Drd2KO (B) of each condition. Scale bars: 100 pA, 20 ms. Bottom: time course of DA effect on D2-MSN evoked IPSCs recorded from D1-MSNs in WT animals in sulp (A, symbols) and from a mixed population of MSNs in iMSN-Drd2KO animals in ACSF (B, pink symbol). The green line shows data from WT in ACSF (Figure 1E). *p < 0.05, paired t tests.

(C) Comparison of DA effect on D2-MSN lateral inhibition in WT in ACSF (green filled) and sulp (green outline) and in iMSN-Drd2KO in ACSF (pink filled) and 50 μM NEM (pink outline) (n = 6–11). *p < 0.05, Tukey's post hoc tests following ANOVA.
(D) Concentration-response curves of DA depression of D2-MSN lateral inhibition in WT and iMSN-Drd2KO. See full curve fit information in Table S1.
(E and F) CV (E) and PPR (F) of oIPSC amplitudes before and during DA at D2-MSN → D1-MSN synapses in WT with sulp and in iMSN-Drd2KO in ACSF (E) (n = 6–9). *p < 0.05, Wilcoxon rank test.
(G) No DA depression of uncaged Rubi-GABA currents on D1-MSNs (n = 5). Top: representative traces of each condition. Scale bars: 50 pA, 50 ms. Bottom: time course (left) and mean IPSC amplitudes before and after DA (right). *p < 0.05 paired t test.
See full statistics in Table S1.

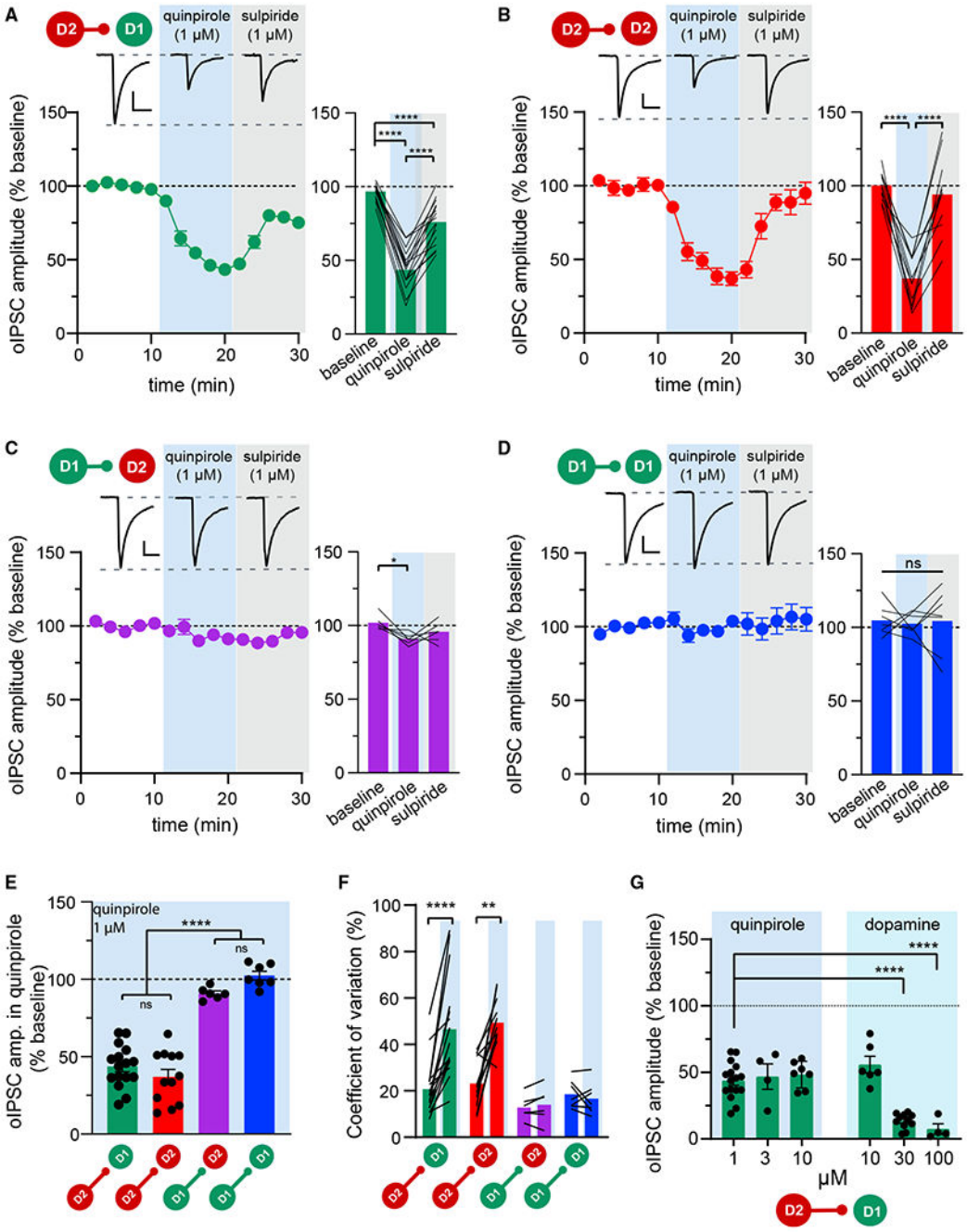

Figure 4. Activation of D2R in presynaptic D2-MSNs depresses lateral inhibition onto other MSNs

(A–D) Effect of quin followed by sulp on D2-MSN→ D1-MSN synapses (A), D2-MSN→ D2-MSN synapses (B), D1-MSN→ D2-MSN synapses (C), and D1-MSN→ D1-MSN synapses (D). Top: representative traces of each condition. Scale bars: 100 pA, 20 ms. Bottom: time course (left) and mean oIPSC amplitudes (right) at baseline, quin, and sulp (n = 16, 12, 6, 7). *p < 0.05, Tukey's test following RM ANOVA.

(E) Quin effect at all MSN synapse combinations. *p < 0.05, Tukey's test following ANOVA.

(F) CV of oIPSC amplitudes at baseline and quin for D2-MSN → D1-MSN (green), D2-MSN → D2-MSN (red), D1-MSN→ D2-MSN (magenta), and D1-MSN → D1-MSN (blue) synapses (n = 16, 12, 6, 7). *p < 0.05, Wilcoxon matched-pairs signed-rank test.
(G) Effect of higher concentrations of quin (n = 16, 4, 7) and DA (n = 6, 11, 6) on D2-MSN → D1-MSN synapses. *p < 0.05, Dunnett's test following ANOVA.
See full statistics in Table S1.

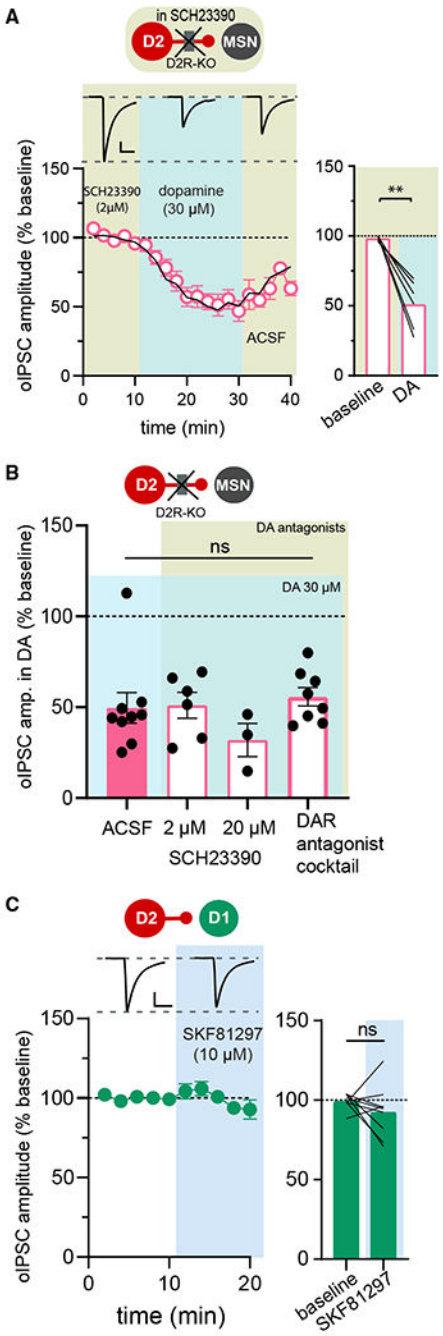

Figure 5. D1Rs are not responsible for D2R-independent depression of D2-MSN lateral inhibition

(A) Effect of DA on D2-MSN → MSN synapses in iMSN-Drd2KO mice in the D1-like antagonist SCH23390 (n = 6). Top: representative traces of oIPSCs of each condition. Scale bars: 100 pA, 20 ms. Bottom: time course of DA effect in SCH23390 (pink) or without (black line; Figure 3B data). Right: mean oIPSC amplitude at baseline and during DA. *p < 0.05, paired t test.

(B) No effect of DA antagonist pretreatment on DA depression of D2-MSN → MSN synapses in iMSN-Drd2KO mice (n = 9, 6, 3, 8). DA antagonist cocktail = 1 μM SKF83566 + 10 μM sulp + 1 μM L-745870. ns, no significant difference; ANOVA.
(C) No effect of the D1-like agonist SKF89217 on D2-MSN → D1 MSN IPSCs in WT mice (n = 9). Top: representative traces of each condition. Scale bars: 400 pA, 50 ms. Bottom: time course (left) and mean oIPSC amplitudes at baseline and SKF89217 (right). Paired t test.
See full statistics in Table S1.

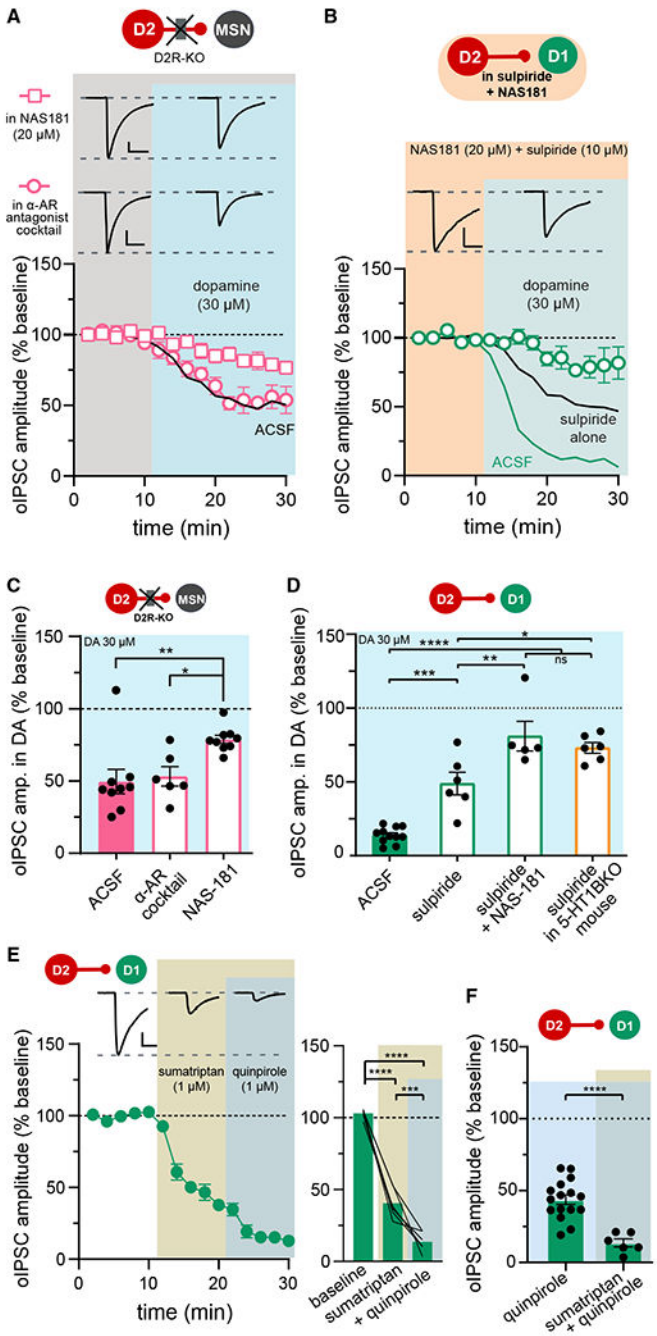

Figure 6. 5-HT1BRs mediate part of the DA depression of D2-MSN lateral inhibition

(A) Effect of preincubation with antagonists for 5-HT1BR or α-AR cocktail on DA inhibition of D2-MSN → MSN synapses in iMSN-Drd2KO mice. Cocktail = yohimbine (3 μM), RX821002 (10 μM), and prazosin (100 nM). Top: representative traces of each condition. Scale bars: 200 pA, 20 ms. Bottom: time course of DA effect with antagonists (symbols) and control (line; Figure 3B data) (n = 9–6).

(B) Effect of NAS-181 + suip on DA inhibition of D2-MSN → D1-MSN synapses in WT. Top: representative traces of each condition. Scale bars: 200 pA, 20 ms. Bottom: time course

in NAS-181 + sulp (symbols), sulp alone (black line; Figure 3A data), or ACSF (green line; Figure 1E data) (n = 5).

(C) Summary of DA effect on D2-MSN → MSN synapses in iMSN-Drd2KO mice (n = 9, 6, 9). *p < 0.05, Tukey's test following ANOVA.

(D) Comparison of DA effect on D2-MSN → D1-MSN synapses in WTmice (green) or in 5-HT1BKO mice with sulp (orange) (n = 9, 6, 5, 6). *p < 0.05, Tukey's test following ANOVA.

(E) Sequential effect of the 5-HT1B/1D agonist sumatriptan and quin on D2-MSN → D1-MSN synapses (n = 6). Top: representative traces of each condition. Scale bars: 100 pA, 20 ms. Bottom: time course (left) and mean oIPSC amplitude at baseline, sumatriptan, and sumatriptan + quin (right). *p < 0.05, Tukey's test following RM ANOVA.

(F) Effects of quin alone and sumatriptan + quin on D2-MSN → D1-MSN synapses (n = 16, 6). *p < 0.05, t test.

See full statistics in Table S1.

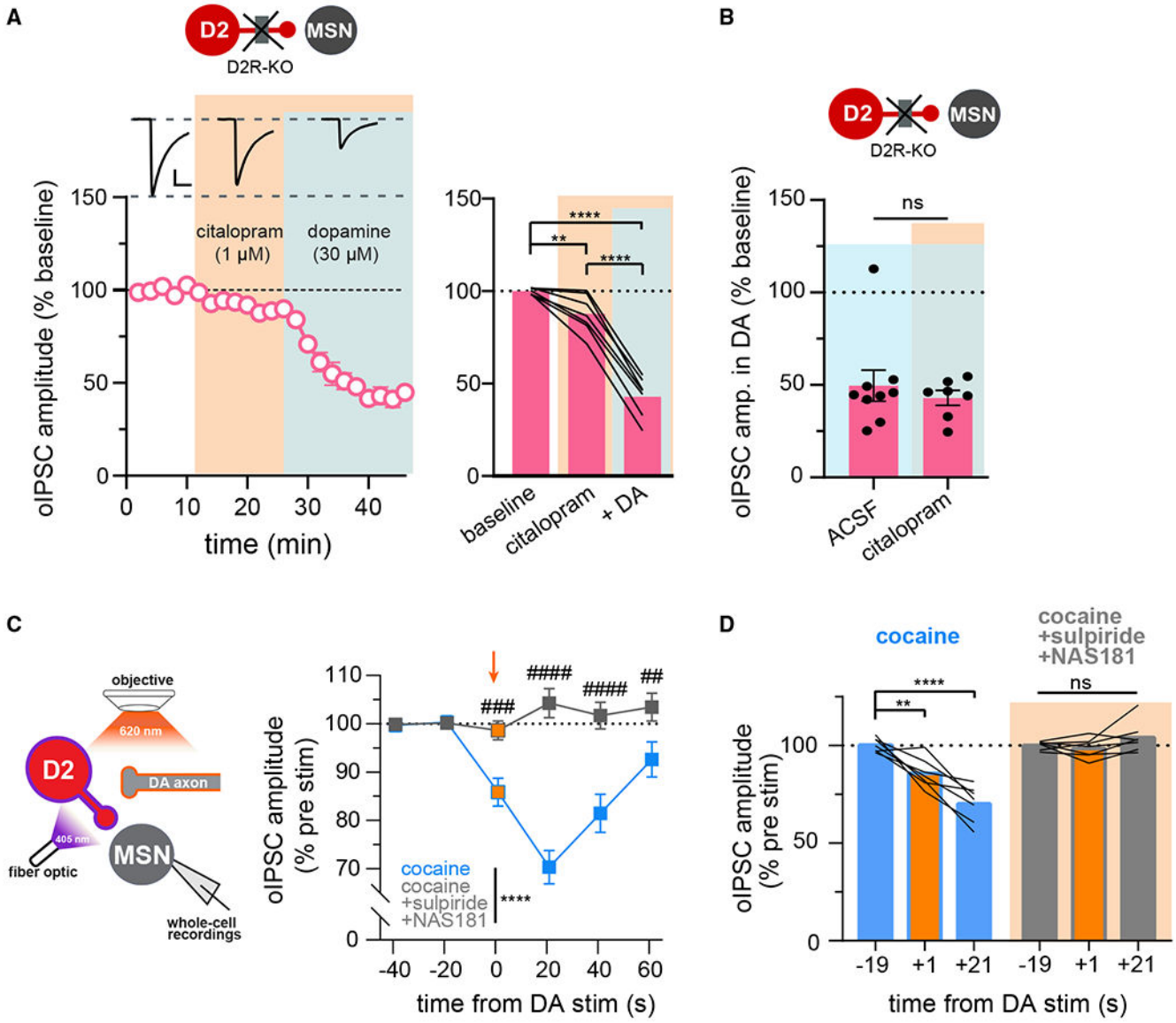

Figure 7. Contribution of endogenous DA, but not 5-HT, to the 5-HT1B-mediated depression of D2-MSN lateral inhibition

(A) Effect of the 5-HT reuptake inhibitor citalopram on DA inhibition of D2-MSN → D1-MSN synapses in iMSN-Drd2-KO mice. Top: representative traces of each condition. Scale bars: 200 pA, 20 ms. Bottom: time course (left) and mean oIPSC amplitude at baseline, citalopram, and citalopram + DA (right) (n = 7). *, significance by Tukey's test following RM ANOVA.

(B) Effects of DA alone and citalopram + DA on D2-MSN → D1-MSN synapses in iMSN-Drd2-KO (n = 9, 7); t test.

(C) Left: dual-color optogenetic stimulation of D2-MSNs and DA axons while recording from MSNs. Center: time course of oIPSC amplitudes at D2-MSN→MSN synapses during endogenous DA release in 3 μM cocaine before (blue) and after (gray) 10 μM sulp + 20 μM NAS-181 (n = 7). Right: oIPSC amplitudes before and after midbrain DA neuron stimulation

were normalized to pre-stimulation (7–10 epochs). Orange symbols show oIPSCs preceded by train stimulation of DA axons. *, significant interaction in 2W RM ANOVA (time × antagonist). #$p < 0.05$, Sidak's test.

(D) Summary oIPSC amplitudes before and 1 s after stimulation (orange), normalized to pre-stimulation, for cocaine (blue) and cocaine + sulp + NAS-181 (gray). *$p < 0.05$, Dunnett's test following RM ANOVA.

KEY RESOURCES TABLE

REAGENT or RESOURCE	SOURCE	IDENTIFIER
Bacterial and virus strains		
ChR2-eYFP (AAV5-EF1a-double floxed-hChR2(H134R)-EYFP-WPRE-HGHpA, $1x10^{13}$ vg/mL	Addgene	Cat# 20298-AAV5; RRID:Addgene_20298
ChR2-eYFP AAV5-EF1a-DIO-hChR2(H134R)-EYFP, $4.5x10^{12}$ vg/mL	UNC Vector Core	Cat# 5EF1aChR2YFPDIO
ChrimsonR-tdTomato (AAV5-Syn-FLEX-rc [ChrimsonR-tdTomato], $5x10^{12}$ vg/mL	Addgene	Cat# 62723-AAV5; RRID:Addgene_62723
Chemicals, peptides, and recombinant proteins		
Dopamine HCl	Sigma	Cat# H8502
NBQX disodium salt	Hello Bio	Cat# HB0443
NBQX disodium salt	Abcam	Cat# ab120046
(R)-CPP	Tocris	Cat# 0247
(R)-CPP	Abcam	Cat# ab120159
Cocaine HCl	NIDA Drug Supply Program	Cat# 9041-001
(RS)-(±)-Sulpiride	Tocris	Cat# 0894
N-Ethylmaleimide	Sigma	Cat# E1271
RuBi-GABA	Tocris	Cat# 3400
(−)-Quinpirole HCl	Tocris	Cat# 1061
SCH 23390 HCl	Abcam	Cat# ab120597
SKF 83566 hydrobromide	Tocris	Cat# 1586
L-745,870 trihydrochloride	Tocris	Cat# 1002
SKF 81297 hydrobromide	Tocris	Cat# 1447
Yohimbine HCl	Abcam	Cat# ab120239
RX 821002 HCl	Tocris	Cat# 1324
Prazosin HCl	Tocris	Cat# 0623
NAS-181	Tocris	Cat# 1413
DPCPX	Tocris	Cat# 0439
Ketanserin tartrate	Tocris	Cat# 0908
Ritanserin	Tocris	Cat# 1955
GR 127935 HCl	Abcam	Cat# ab120523
Methysergide maleate salt	Sigma	Cat# M137
Scopolamine hydrobromide	Tocris	Cat# 1414
AM251	Tocris	Cat# 1117
CGP 55845 HCl	Hello Bio	Cat# HB0960
Naloxone HCl	Tocris	Cat# 0599
SR95531 (Gabazine)	Abcam	Cat# ab120042
Kynurenic acid sodium salt	Hello Bio	Cat# HB0363
Kynurenic acid	Sigma	Cat# K3375

REAGENT or RESOURCE	SOURCE	IDENTIFIER
Citalopram	Abcam	Cat# ab120133
Sumatriptan succinate	Tocris	Cat# 3586
Experimental models: Organisms/strains		
Mouse: Drd1-tdTomato (B6.Cg-Tg(Drd1a-tdTomato)6Calak/J)	The Jackson Laboratory	JAX: 016204; RRID:IMSR_JAX:016204
Mouse: Adora2a-Cre (B6.FVB(Cg)-Tg(Adora2a-Cre)KG139Gsat/Mmucd)	MMRRC	MMRRC: 036158-UCD; RRID:MMRRC_036158-UCD
Mouse: Drd1-Cre (B6.FVB(Cg)-Tg(Drd1-Cre)EY262Gsat/Mmucd)	MMRRC	MMRRC: 30989-UCD; RRID:MMRRC_030989-UCD
Mouse: DAT-Cre (B6.SJL-Slc6a3$^{tm1.1(cre)Bkmn}$/J)	The Jackson Laboratory	JAX: 006660; RRID:IMSR_JAX:006660
Mouse: D2$^{loxp/loxp}$ (B6.129S4(FVB)-Drd2$^{tm\ 1.1Mrub}$/J	The Jackson Laboratory	JAX: 020631; RRID:IMSR_JAX:020631
Mouse: 5HT1B$^{-/-}$(C.129-*Htr1b*^{tm1Rhn}/MpenJ)	Dr. John Williams, Vollum Institute	JAX: 029609; RRID:IMSR_JAX:029609
Software and algorithms		
pClamp 10 (acquisition: 10.3; analysis: 10.7)	Molecular Devices	https://www.moleculardevices.com/
Prism (8.3.1)	Graphpad Software	https://www.graphpad.com
Illustrator (25.2.3)	Adobe	https://www.adobe.com
Excel (16.0.13127.21490)	Microsoft	N/A
Igor Pro 8 (8.0.3.3)	WaveMetrics	https://www.wavemetrics.com/